Evaluating innovative collective heating and cooling concepts by incorporating occupants' preferences for conflicting performance indicators

Reference:
Jacobs Stef, Van Minnebruggen Senne, Matbouli Houssam, Ghane Sara, Hellinckx Peter, Verhaert Ivan.- Evaluating innovative collective heating and cooling concepts by incorporating occupants' preferences for conflicting performance indicators
Energy and buildings - ISSN 1872-6178 - 314(2024), 114264
Full text (Publisher's DOI): https://doi.org/10.1016/J.ENBUILD.2024.114264
To cite this reference: https://hdl.handle.net/10067/2057950151162165141

Graphical Abstract

Evaluating Innovative Collective Heating and Cooling Concepts by Incorporating Occupants' Preferences for Conflicting Performance Indicators.

Stef Jacobs, Senne van Minnebruggen, Houssam Matbouli, Sara Ghane, Peter Hellinckx, Ivan Verhaert

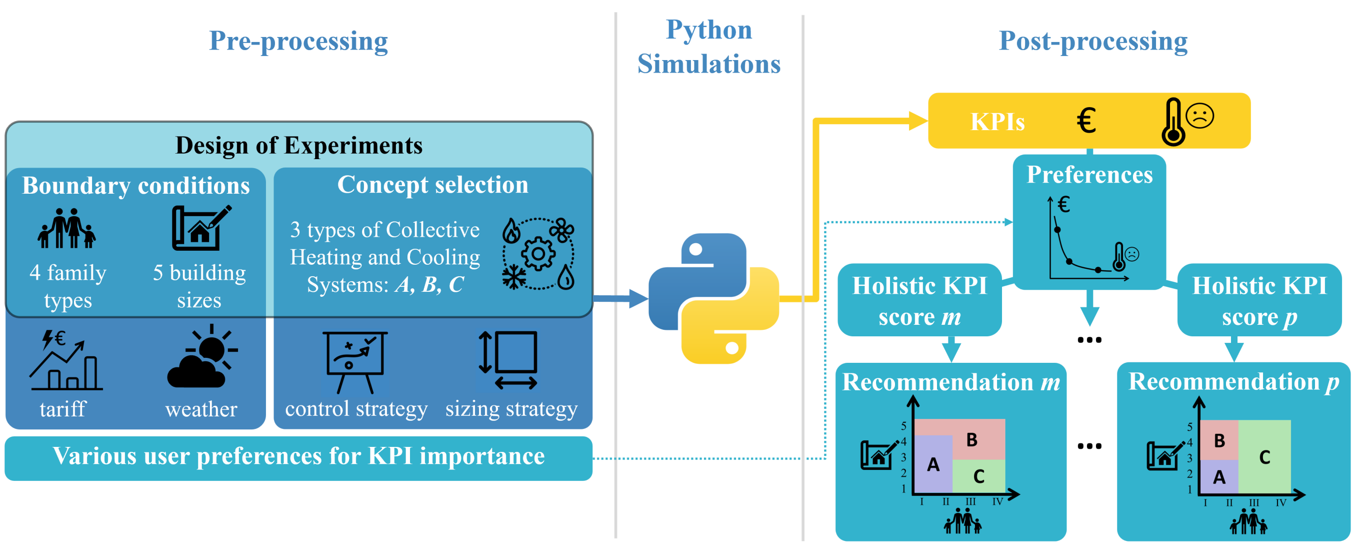

Highlights

Evaluating Innovative Collective Heating and Cooling Concepts by Incorporating Occupants' Preferences for Conflicting Performance Indicators.

Stef Jacobs, Senne van Minnebruggen, Houssam Matbouli, Sara Ghane, Peter Hellinckx, Ivan Verhaert

- Introduction of holistic KPI score for multi-objective and user-based evaluation.
- General selection methodology to compare collective heating and cooling concepts.
- Demonstration on a Flemish case study for three central change-over concepts.
- 4-pipe system is recommended when focus lies on thermal comfort.
- Decentralised booster heat pumps have the lowest ratio of costs to energy use.

Evaluating Innovative Collective Heating and Cooling Concepts by Incorporating Occupants' Preferences for Conflicting Performance Indicators.

Stef Jacobs[a,b,*], Senne van Minnebruggen[a], Houssam Matbouli[a], Sara Ghane[c], Peter Hellinckx[b], Ivan Verhaert[a]

[a] *EMIB, Faculty of Applied Engineering - Electromechanics, University of Antwerp, Groenenborgerlaan 171, Antwerp, 2020, Belgium*
[b] *M4S, Faculty of Applied Engineering - Electronics ICT, University of Antwerp, Groenenborgerlaan 171, Antwerp, 2020, Belgium*
[c] *University of Antwerp - imec, IDLab - Faculty of Applied Engineering, Sint-Pietersvliet 7, Antwerp, 2000, Belgium*

Abstract

Various Collective Heating and Cooling Systems (CHCS) have emerged as promising low-carbon energy solutions for buildings. However, the absence of tailored decision guidelines often hinders decision-makers from identifying the optimal system for any given case. This research introduces a novel methodology for comprehensive evaluation of different CHCS under diverse case-specific boundary conditions, leading to informed recommendations. The proposed methodology integrates occupants' preferences for thermal comfort and costs into a holistic Key Performance Indicator (KPI) score, i.e. a weighted sum of normalised indicators including indoor thermal comfort, domestic hot water comfort, and levelised cost of energy. By applying this methodology to evaluate three advanced central change-over temperature CHCS across various building sizes and family types, our study demonstrates the effectiveness of this approach. The results suggest that 4-pipe systems are preferable when prioritising thermal comfort, whereas decentralised booster heat pumps are recommended for cost reduction. Notably, for small apartment buildings inhabited by working families, a 2-pipe system with decentralised storage might be preferred. These insights underscore the importance of incorporating occupants' preferences into multi-objective decision-making. Furthermore, the holistic KPI score methodology can assess different control strategies and provide valuable insights for policymakers when extended with additional indicators.

Keywords: Collective heating and cooling, Central change over systems, Heat pump, Electrification, Evaluation framework, Multi-objective

1. Introduction

Collective heating systems play a crucial role in realising the 2050 climate objectives [1, 2] by facilitating a sustainable energy supply across multiple energy vectors [3]. These systems accommodate diverse heat demands, including Space Heating (SH) and Domestic Hot Water (DHW), for various end-users through shared production units and extensive distribution networks [4]. The substantial reduction in temperature levels in the recent decades [5, 6] has improved the efficiency of these systems and enabled the integration of a broader range of renewable and low-exergy sources [7], aligning with the key criteria for energy decarbonisation by 2050 [8].

In the broader context of collective heating, the need to address Space Cooling (SC) supply alongside efficient heat supply has become increasingly evident due to increased insulation rates and climate change [9, 10]. Certain mitigation strategies, such as solar shading, have demonstrated potential in mitigating the increase in building cooling demand. However, it is anticipated that building cooling demand will experience substantial growth by mid of 21st century across various climates: 33% in tropical regions, 89% in arid climates, 288% in cold climates, and 376% in temperate regions [11]. Specifically, dense urban areas, influenced by the urban heat island effect, are experiencing a rise in cooling demand [12]. Individual air conditioning units, commonly used in urban areas, reinforce the heat island effect which highlights the necessity for sustainable alternatives.

The integration of SC supply within collective heating systems efficiently addresses both SH and SC demands across various dwellings [13]. Considering that 78% of residential heat demand in Europe is concentrated within just 1.4% of the land area [14], underscores the significant opportunity to implement collective heating and cooling systems. Thermal systems aiming to fulfill both heating and cooling demands of connected end-users in residential apartment buildings are hereinafter referred to as Collective Heating and Cooling Systems (CHCS).

In the drive to optimise CHCS, a myriad of concepts are available and new ones are being researched. For example, the aim to reduce distribution temperatures has led to systems with a distribution temperature control strategy to switch between different temperature levels, i.e. central change-over systems [15]. These also include multiple distribution pipes to facilitate different temperature levels simultaneously or (decentralised) booster systems combined with low central distribu-

*Corresponding author
Email addresses: Stef.Jacobs@uantwerpen.be (Stef Jacobs), Senne.VanMinnebruggen@uantwerpen.be (Senne van Minnebruggen), Houssam.Matbouli@uantwerpen.be (Houssam Matbouli), Sara.Ghane@uantwerpen.be (Sara Ghane), Peter.Hellinckx@uantwerpen.be (Peter Hellinckx), Ivan.Verhaert@uantwerpen.be (Ivan Verhaert)

tion temperatures [16, 17]. However, the efficiency of central change-over CHCS is strongly correlated to the characteristics of the demand profiles [15]. Therefore, evaluation frameworks that take account of these factors are required and should be used to give recommendations to decision-makers and stakeholders during the selection of a CHCS.

1.1. Assessment Frameworks for Collective Heating and Cooling Systems

For assessing heating networks, Vering et al. [18] recommend a simulation-based evaluation framework. It considers nonlinear inter-dependencies during operation and facilitates systems sizing (and control) optimisation. Moreover, it ensures an objective evaluation by maintaining consistent boundary conditions when assessing different CHCS concepts at an early stage. Additionally, these boundary conditions can be adapted to study their influence on Key Performance Indicators (KPIs), allowing selection recommendations to be adjusted.

In general, existing simulation-based evaluation frameworks can be divided into two groups. On the one hand are the evaluation frameworks that focus on assessing control strategies. For example, Blum et al. [19] developed a standardised evaluation framework, named BOPTEST, for different control strategies. Although such a standardised approach is beneficial for objective comparison of new control methodologies in standardised concepts [20], it cannot be used for evaluating novel concepts across different boundary conditions. Jacobs et al. [15] used an assessment framework to introduce and evaluate control strategies for grouped charging of decentralised storage tanks. Although the effects of sizing and control are considered for a scalable case study, the novel concept is not compared to other state-of-the-art CHCS for various occupant behaviours and preferences.

On the other hand are the evaluation frameworks that focus on evaluating concepts and their designs. For example, Wang et al. [21] compared different collective cooling concepts in China. They endorsed that weather conditions are important in the selection, but their evaluation did not assess the influence of different building types and user profiles. Benakopoulos et al. [22] presented a general overview of possible concepts for DHW production with low-temperature DH. Their focus was on the DHW circulation circuit of 4-pipe systems in an apartment building, but the effects of occupant behaviour, sizing and building types were not discussed. Debacker et al. [23] performed a financial evaluation for newly built, single-family buildings in Belgium. Here the relative importance of different costs were found to influence the best selection for the heating and cooling system. Allouhi et al. [24] used a multi-objective optimisation to determine the most optimal collector area, hot water tank volume and photovoltaic capacity for a solar power-to-heat system. In the optimisation, the focus lied in financial KPIs and the geometric distance between the simulated concepts and the idealised, non-realistic system in the Pareto front was minimised. Furthermore, the Energy Performance of Buildings Directive (EPBD) legislation [25] significantly impacts the system selection in buildings. Each European country has its own software, based on this EPBD legislation, to assess the energy performance of buildings. However, these software tools are based on a myriad of correction factors and typically incorporate only conventional concepts. In Belgium, a conformity certificate can be utilised to evaluate innovative systems, such as central change-over systems. However, this approach lacks a standardises evaluation, leading to an underestimation of the performance of new systems. Additionally, the simulation time steps of one month overlook the impact of control strategies, which is crucial for central change-over systems.

Other studies included the effects of building types on concept selection into their evaluation framework for concepts and their designs. For example, Dermentzis et al. [26] conducted an energetic evaluation of nine HP-based (collective) heating concepts across three renovation levels for a theoretical apartment building. However, the impact of occupant behaviour on the system performance was not investigated and only the annual electricity consumption over the total heat demand per floor area was used for evaluation. Another comparative analysis of collective heating systems is presented by Martinopoulos et al. [27] that included a theoretical 3-floor apartment building in different Mediterranean climates. Here, the focus was on the financial evaluation of systems and they concluded that location affects the optimal system selection.

Additionally, different evaluation frameworks typically utilise different KPIs which makes the comparison across different studies difficult. Therefore, Abbasi et al. [28] selected the 22 most used sustainability indicators based on a thorough literature review that focuses on environmental, social and economical aspects. They concluded that the environmental aspects should cover the largest part of an evaluation framework, with CO_2 emissions and primary energy use as main indicators. In terms of economical evaluation, the net present values and operational costs are determining for decision-makers. The insights of Jafaryeganeh et al. [29] help to cope with multi-objective decision-making efficiently. The primary conclusion drawn from this literature review is that different KPIs should undergo normalisation to be dimensionless before applying a multi-objective decision method, which is mostly based on weighted sum.

1.2. Problem Statement: Central Change-Over CHCS

As can be noted, assessing and comparing different CHCS poses a major challenge due to numerous factors involved, including building characteristics, occupant profiles, weather conditions, component sizing, implemented control strategy, among others [30]. As a result, it is not clear for decision-makers which CHCS to select for a specific case, certainly not for the novel central change-over systems. In this respect, performing a comparative analysis for different boundary conditions gives insights into the optimal application domain of different central change-over CHCS, which can lead to generating informed recommendations.

With respect to the KPIs used to generate these recommendations, it is essential to incorporate (future) occupants' preferences for conflicting KPIs, such as thermal comfort and operational cost [28]. Thermal comfort directly affects occupants' well-being and satisfaction. Simultaneously, operational cost impacts the system's economic sustainability and occupants' financial satisfaction. Balancing the comfort and costs is critical for optimal system design and aligns with occupant-centered building practices.

This underscores the necessity to develop a comprehensive evaluation framework for CHCS that accounts for boundary conditions and a method that accounts for the preferences of occupants regarding conflicting KPIs into the multi-objective decision-making. This method aims to facilitate informed recommendations tailored to various cases.

1.3. Scope and Contributions of the Paper

In this manuscript, we present a novel performance-based evaluation method for informed decision-making. The purpose of this method is to assess and compare variants of Collective Heating and Cooling Systems (CHCS) across diverse boundary condition scenarios. Notably, the evaluation method goes beyond conventional approaches by incorporating occupants' preferences regarding thermal comfort and costs into the multi-objective assessment. This enables to generate informed recommendations that consider subjective considerations.

The method is demonstrated through the generation of recommendations for central change-over systems that switch several times a day between different temperature levels to meet SH, SC and DHW demands. To achieve this, the evaluation method is implemented into a comprehensive evaluation framework that considers influential factors such as building characteristics, occupant profiles, component sizing and different control strategies. The paper contributes significantly to the research field of CHCS in apartment buildings in two main ways:

1. **Holistic Key Performance Indicator score (KPI^*):** The use of a holistic KPI score marks a notable departure from conventional assessment frameworks. This enables the integration of occupants' preferences concerning a multi-objective evaluation problem to generate CHCS selection recommendations. This approach facilitates the identification of the most suitable CHCS for diverse boundary conditions, offering an improvement in decision-making frameworks.
2. **Evaluation of three novel central change-over CHCS:** The proposed methodology is demonstrated through the evaluation of three state-of-the-art central change-over temperature CHCS for various building sizes and occupant behaviour profiles. The investigated CHCS include (see Section 2.3) a booster heat pump-based 2-pipe system, a 2-pipe system with decentralised storage, and a 4-pipe system, offering insights into their application potential. Because of ongoing electrification of thermal energy, all generation units are Power-to-Heat solutions.

The rest of this paper is organised as follows: the novel evaluation methodology with the structure of design of experiments, the three evaluated central change-over CHCS concepts, and the simulation environment are described in Section 2; Section 3 first presents the case-specific inputs to demonstrate the methodology for generating informed recommendations tailored to varied boundary conditions and various occupants' preferences. Afterwards, it provides a discussion on the proposed methodology; and the paper concludes in Section 4.

2. Material and Methods

2.1. Overall Evaluation Framework

This study aims to introduce a general methodology for generating recommendations on CHCS selection based on dynamic simulations in Python. These recommendations account for occupants' preferences regarding conflicting KPIs. Tailored recommendations are provided based on specific boundary conditions, meaning that the recommended CHCS may vary based on factors such as the region considered or occupant behaviour profile. Figure 1 provides a schematic representation of the evaluation framework, comprising pre-processing, python simulations and post-processing.

During the pre-processing phase, the evaluation methodology is structured around defining the design of experiments to generate tailored recommendations by specifying required inputs. These inputs can be broadly categorised into boundary conditions and concepts under evaluation, each serving distinct roles within the evaluation framework. Boundary conditions, which include i occupancy profiles, j building characteristics, k energy tariff structures, and l weather profiles, are case-specific parameters that form the contextual foundation for the evaluation. Their adaptability allows for easy adjustment to accommodate various real-world scenarios. In addition, the Z concepts under evaluation encompass U different CHCS, V control strategies and W sizing strategies embedded in the CHCS. These investigated concepts are also adaptable, but the incorporation of novel systems or strategies into the evaluation framework requires careful adaptation into the Python simulation environment. Therefore, Section 2.2 outlines the required inputs for defining boundary conditions, while Section 2.3 introduces the central change-over CHCS along with the sizing and control strategies used in demonstrating this methodology.

The Python simulation environment, built upon previous research (see Section 2.4), produces results that are translated into financial KPIs and thermal comfort KPIs (see Section 2.5.1) during post-processing. While CO_2 or primary energy consumption are recommended KPIs by [28], they are not included in this research to maintain focus on proposing a decision-making method that integrates occupants' preferences.

The trade-off between these KPIs is typically visualised by a Pareto front, yet this does not simplify the CHCS selection process. To take account of occupants' preferences, a holistic KPI score (described in Section 2.5.2) is proposed. This approach enables the systematic generation of tailored recommendations by exploring the interplay between different boundary conditions and the diverse concepts under investigation. For instance, the design of experiments may entail examining various configurations of CHCS or exploring alternative control and sizing strategies tailored to specific CHCS configurations for diverse boundary conditions.

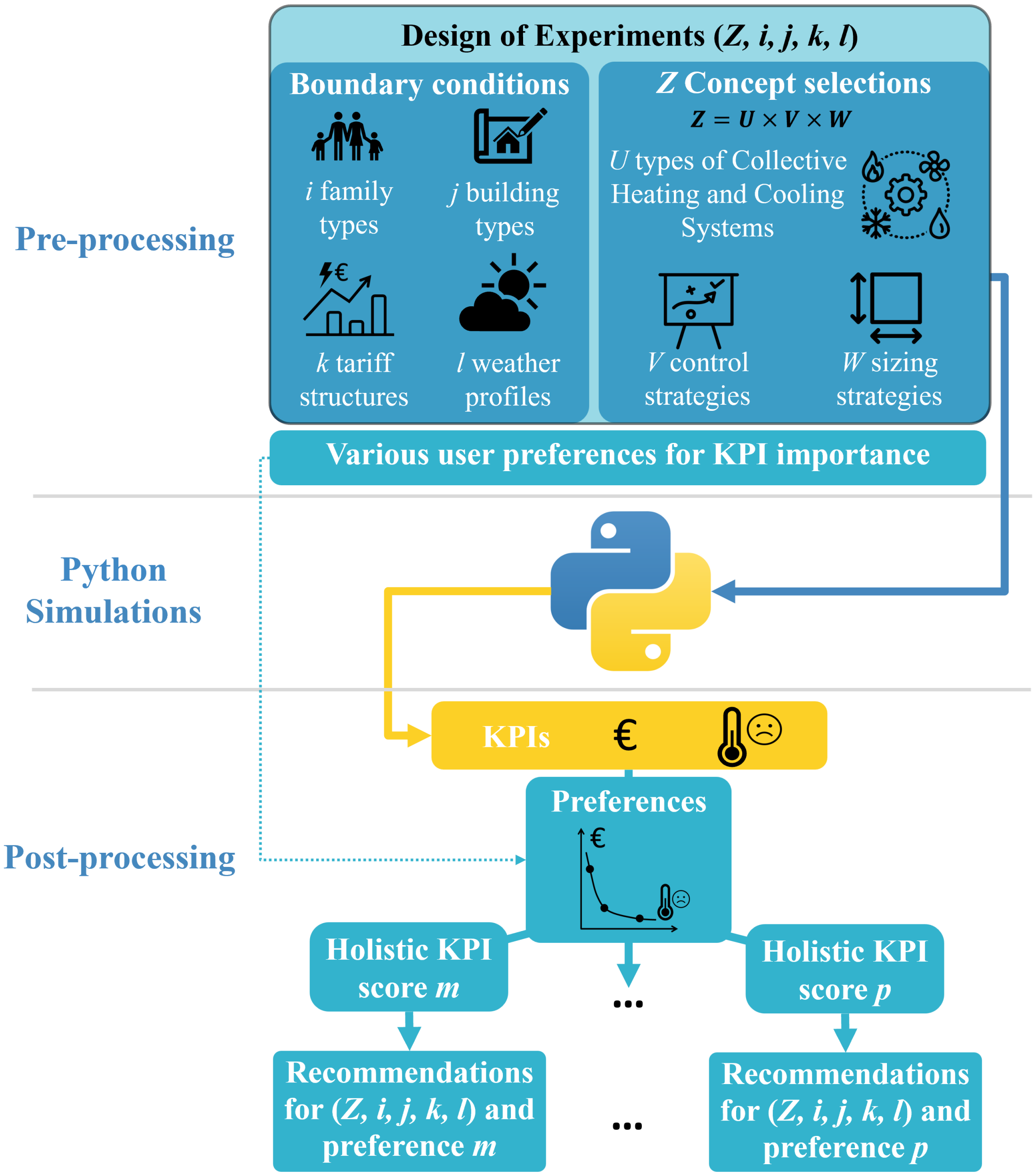

Figure 1: Schematic overview of methodology. The design of experiments can include i different family types, j building types, k tariff structures and l weather profiles. Recommendations are generated based on these variations in boundary conditions to select the optimal CHCS, control strategy and/or sizing strategy, considering preferences toward conflicting KPIs.

2.2. Boundary Conditions

This section provides a general overview of the required case-specific inputs essential for defining the boundary conditions, which form the basis for the recommendations. Detailed parameters for demonstrating the proposed evaluation methodology are presented in Section 3.1.

2.2.1. Weather Conditions

The weather data files serve as essential for conducting comparative analyses as they represent the geographical location under consideration. These files, integrated into the simulation environment, must contain outdoor temperature measurements [°C] and solar radiation measurements [W/m²], for each cardinal direction: North, East, South and West. When the time step of the data file does not align with the simulation time step, linear interpolation is applied to ensure compatibility.

Although full year simulation data is typically available, the small simulation time step and the detailed models (described in Section 2.4) would result in extended simulation times when conducting diverse experiments. Consequently, a compromise was made between computational efficiency and obtaining detailed annual results.

To assess the year-round performance of the considered CHCS, representative months are selected to cover a range of typical climatic challenges throughout the year. The simulation results from these representative months are extrapolated to annual KPIs based on a weighted sum. This method, similar to the approach described in [31], classifies the remaining months based on similarity to the representative months.

An illustrative example with three operation modes is shown in Figure 2, where January signifies a typical winter month (in red), July a typical summer month (in blue), and the period from September 15 to October 15 a typical spring/autumn month (in green). The coloured boxed at the bottom denote which months correspond to which of these three representative months.

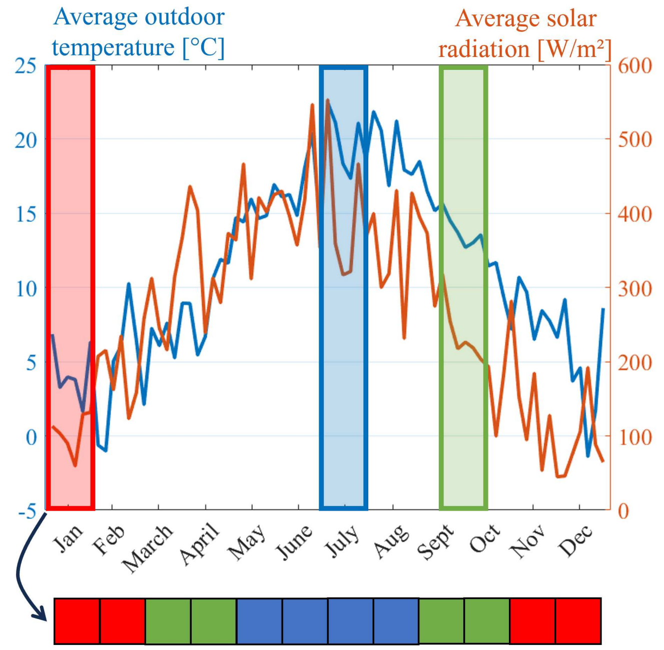

Figure 2: Example of a weather profile. Here, the weather conditions (average outdoor temperature [°C] and average sum of solar radiation [W/m²]) are shown. The boxes visualise how the year performance is derived from three representative months.

2.2.2. Tariff Structure

The tariff structures need to be defined for all energy sources in €/kWh. These structures may encompass fixed tariffs for gas and electricity or exhibit variability over time, such as monthly prices or even day-ahead market prices for electricity. When calculating the operational costs for a non-simulated month based on a representative month, it is imperative to consider the price of that non-simulated month according to the used profile. Consequently, a daily or hourly price setting is only feasible when simulating the entire year without relying on representative month distribution, resulting in increased simulation times.

2.2.3. Building Characteristics

This research employs a conceptual apartment building designed as a modular assembly of 14 distinct dwelling configurations. These configurations are allocated across different levels within the apartment building, encompassing the floor level, the top level, or an intermediate level. Notably, this method of assembling building configurations allows for adaptable scenarios, facilitating the selection of specific configurations in varying quantities.

Each configuration is characterised by a set of parameters reflecting transmission losses, ventilation losses, and solar gains. These parameters encompass total floor area [m²], dwelling height [m], total loss area of walls [m²], U-value of walls [W/m²K], as well as windows and ventilation characteristics. Window characteristics include glass area for the four cardinal directions [m²], U-value [W/m²K], and solar radiance transmission factor. Ventilation parameters necessitate the definition of the ventilation system (mechanical or natural, balanced or unbalanced and heat recuperation efficiency), ventilation rate [m³/h], and air leakage rate for both winter and summer conditions, for instance, in summer for free cooling via night ventilation.

The scalable nature of the conceptual apartment building allows for variation in the number of dwellings within the apartment building to generate recommendations. It is noteworthy that although 14 dwelling configurations are predetermined, expansion is feasible by defining alternative values for these parameters.

2.2.4. Occupant behaviour Profiles

Besides the building characteristics, the occupant profiles are determining for the system efficiency by affecting energy consumption and number of central supply temperature switches. Occupancy is stochastic in nature with varied patterns for each dwelling, leading to diverse schedules and requirements for heating and cooling. The stochastic profile generator, developed in the Instal2020 project [32], is used to generate various occupant behaviour profiles. These profiles consists of internal heat gains [W], occupancy presence, DHW consumption [kg/s] at 60°C, and zone temperature set point schedules. This generator allows to choose for each dwelling between nine different family types, ranging from 1 to 4 inhabitants, and the number and type of tapping points [33]. The nine family types, described in [33], result from a survey held on 700 dwelling in Belgium during the Instal2020 project.

2.3. Selected Collective Heating and Cooling System Design

In addition to defining boundary conditions, which provide the foundation for recommendations, the concepts under evaluation must be specified during the pre-processing stage. The design process for CHCS involves three main steps: concept selection, concept sizing, and implementing a control strategy. Unlike boundary conditions, these inputs require careful coding for integration into the evaluation framework. Therefore, this section immediately describes the considered concept selections, sizing and control strategies that are subject to demonstration of the methodology. For this demonstration, three central change-over CHCS are compared across varied boundary conditions, utilising sizing and control strategies based on easily implementable methods derived from scientific literature. It is important to note that the methodology outlined here is not limited to the evaluation of these specific concepts but is applicable to comparing other concepts, as well as different control and sizing strategies within a certain CHCS design.

2.3.1. Selection of Concept

As only newly built apartment buildings are considered in this research, all dwellings are equipped with an underfloor system for heating that can switch to underfloor cooling. Their design temperature is set at 35°C/30°C for heating. A passive mixing valve incorporated in any underfloor system regulates the inlet temperature to a maximum of 35°C.

In the central production only power-to-heat solutions are considered to align with the need for electrifying the thermal energy supply. Therefore, the principal heat generator is always a geothermal heat pump (GHP), connected to a Thermal Energy Storage (TES) with two temperature sensors set at 45 °C. The geothermal source is a Borehole TES (BTES), which enables free-cooling in summer by means of a plate heat exchanger between supply and BTES, bypassing the GHP. In case a central high-temperature unit is required for supplying higher temperatures than 45 °C, a High-Temperature HP (HT-HP) is put in series, which is also connected to a TES. This way, the temperature can also increase to 65 °C for production of DHW in concepts A and C. The series connection is the preferred setup when the principal heat generator is a HP [34].

The three considered central change-over CHCS are referred to as concept A, B and C are also shown in Figure 3:

A) The new 2-pipe concept with decentralised storages for DHW and central change-over system, as presented in [15]. The decentralised storages are charged simultaneously as much as possible to allow both high temperature (for storage charging) and low temperatures (for SH or SC) distribution.

B) A prosumer-based 2-pipe CHCS with decentralised booster heat pumps (BHP) represents an emerging variant of 2-pipe systems. In this configuration, the distribution temperature can be easily adjusted and switched between SH and SC on an hourly basis. The DHW is produced locally, with the BHPs utilising central heat from the supply pipe as a heat source. Consequently, a central HT-HP is not required in this system.
During summer months, excess heat within apartments can be utilised for local DHW production, facilitated by an intelligent heat recuperation system (blue pipes in Figure 3**b**) as shown by Jacobs et al. [35]. The key principle involves connecting the SC outlet temperature (which is warmer than the supply pipe temperature) to the evaporator of the BHP. This results in an increase in the source temperature of the BHP, thereby enhancing its COP. Additionally, the cold return water from the evaporator can serve as a cooling source for the underfloor system.

C) The third concept is a 4-pipe system, where one distribution circuit is designated to supply SH and SC, while the second circuit distributes DHW. In theory, this concept should deliver the highest comfort level for DHW, as DHW supply is always available. However, supplying the high temperature at all times reduces the energy efficiency due to high heat losses and lower production efficiency of central HP. The central TES of the HT-HP contains an internal spiral heat exchanger for producing DHW. The circulation loop is connected to this TES.

2.3.2. Component Sizing

The sizing predominantly adheres to established sizing methodologies, although certain specific concepts lack a proven optimal sizing strategy. This section first delves into the sizing of components within dwellings, followed by a discussion on the sizing of central production units.

In all concepts, the sizing of the underfloor heating system is based on the design heat demand, utilising a regime temperature of 35°C/30°C. For concepts A and B, the volumes of decentralised storage tanks are determined using the 'Power-Storage'-method introduced by Verhaert et al. [36], given a certain heating power. Figure 4 visualises this method, where the peak cumulative demand for DHW within different time step intervals for an average dwelling is shown in purple. The black curve represents the cumulative heat delivered by a DHW production continuously heating at its nominal heating power during the same time step intervals. The required storage volume is derived from the largest difference between these two graphs. Note that determining the required storage volume using the 'Power-Storage'-method [36] requires first defining the heating power.

The heating power of the decentralised DHW production varies depending on the employed concept. For concept A, the heating power relies on the internal coil heat exchanger. Assuming a charging flow rate of 300 kg/h, as was considered

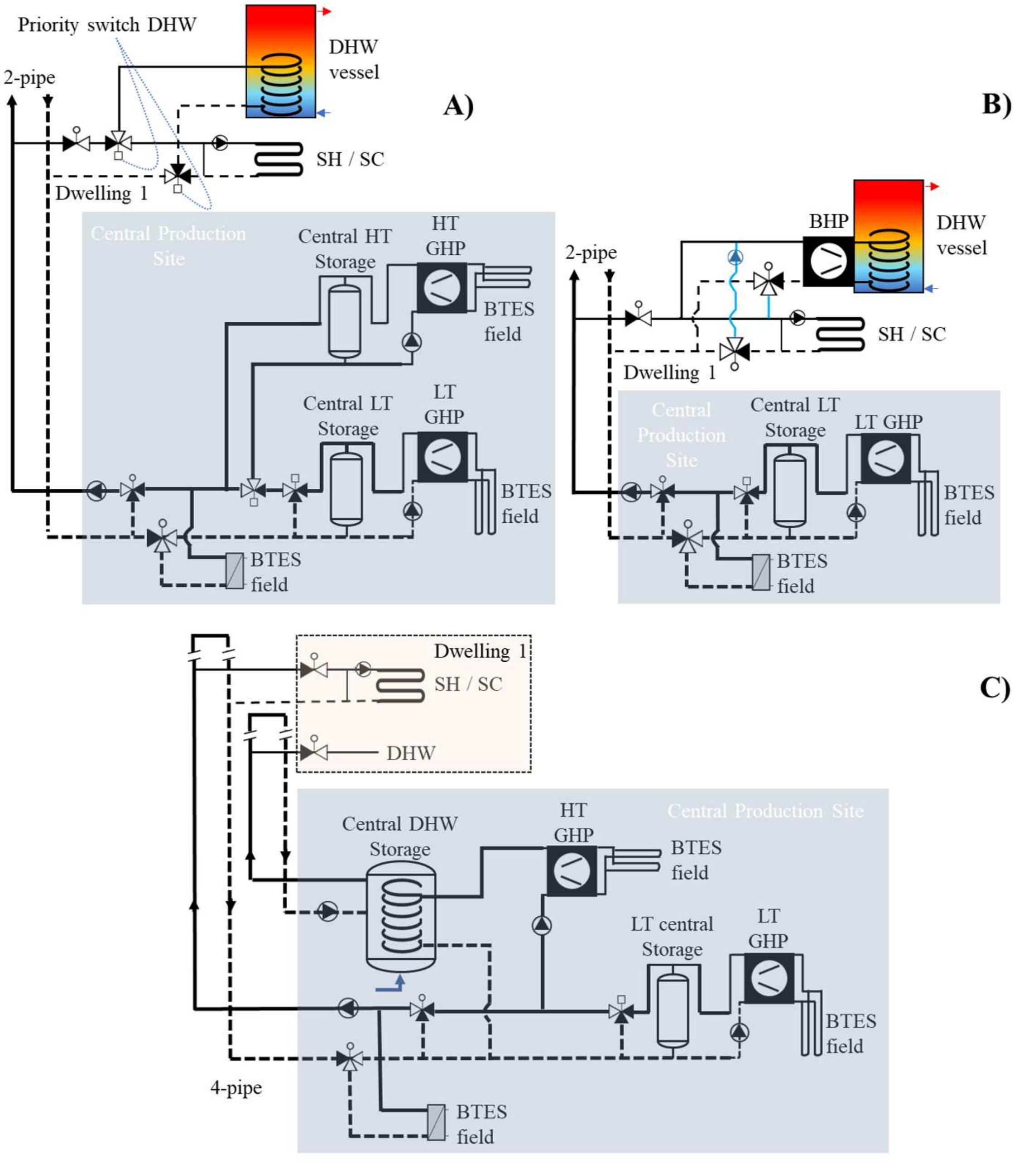

Figure 3: Schematic overview of the three central change-over CHCS, (**A**) 2-pipe system with decentralised storage tanks, (**B**) 2-pipe system with decentralised booster heat pumps, and (**C**) 4-pipe system.

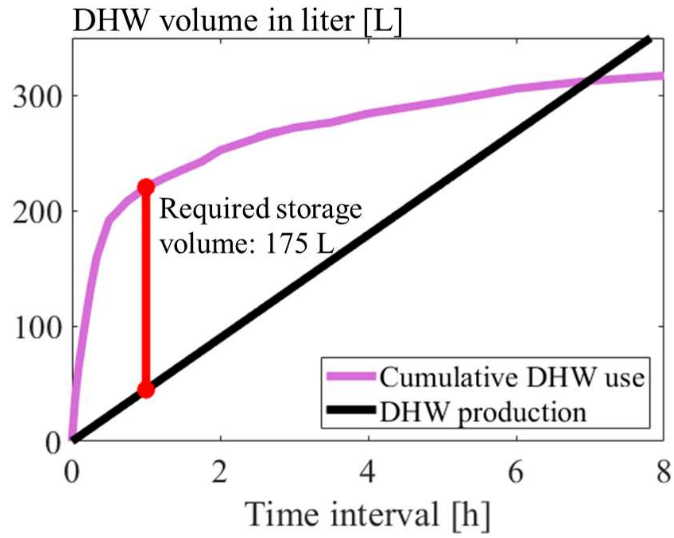

Figure 4: Example of DHW storage volume calculation for an apartment building. The purple line represents the average of all peak cumulative DHW demands of all dwellings for different time step intervals. The black line is the produced DHW during those time intervals. The maximum difference between these two lines equals the required storage capacity in liter to provide DHW comfort. In this example, the production unit has a heating power of 2500 W, resulting in a required storage tank volume of at least 175 litres.

ideal by the sizing study conducted by Jacobs et al. [15], and a 10°C average temperature difference, the charging power is 3.5kW. For concept B, the assumed heating power is 2kW by default, aligning with typical specifications of DHW booster heat pumps in the market.

In all three concepts, the associated TES for the GHP has a storage volume equivalent to one hour of full-load operation of the GHP, as identified as the most efficient by Van Riet [34]. The central GHP is sized to meet the space heating demand for all dwellings, averaging 2kW per dwelling. Only in case of BHPs (concept B), the GHP is sized 30% larger. This 30% increase accounts for the extra heat extracted by decentralised BHPs, assuming an average Coefficient of Performance of 4.2 for BHPs [35], BHPs of 2kW, and a simultaneity of 40%.

For concepts A and C, the sizing method diverges for the central HT-HP. In concept A, the HT-HP is sized with design temperatures at condenser side of 45°C/65°C and a flow rate of $S \times 300$ kg/h, where S represents the simultaneity factor of DHW demand in the dwellings [37]. In concept C, the flow rate is determined by the average peak demand of all dwellings in a 10-minute time interval, multiplied by $S \times 0.7$. The central DHW storage volume of concept C is defined based on the 'Power-Storage'-method, similar to the sizing of decentralised DHW storages.

2.3.3. *Control Strategies*

The control strategies implemented in the three CHCS are derived from previous researches or are adapted for this research, with a focus on adopting easily implementable rule-based control strategies.

Each of the central change-over CHCS need to switch between SH and SC, with an additional temperature level of DHW production in concept A. In concept B, DHW is locally produced with the BHP, while in concept C, DHW distribution occurs through a separate circuit.

The strategy for switching between SH and SC remains consistent across all three concepts. This rule-based control strategy requires meeting three conditions before the system can switch from heating mode to cooling mode. Firstly, the average outdoor temperature of the past 24 hours must exceed 15°C, representing the activation of summer mode. Secondly, the operative temperatures of all dwellings must be maintained above the indoor operative temperature set point ($T_{op;SP}$), to prioritise space heating in the building. Lastly, a minimum of 33% of dwellings must have an operative temperature higher than the set point for space cooling.

In concept A, the described switching strategy between SH and SC has been combined with the two-sensor control (2SC) of [15]. The 2SC relies on two temperature sensors in each decentralised storage tank to determine whether the central supply temperature should be increased to 65°C (DHW mode) or not. The central supply temperature switches between 65°C (DHW mode), 35°C (SH mode) and 18°C (SC mode).

For concept B, the central supply temperature should be as low as possible during SH [35], and as high as possible during space cooling. Therefore, a fixed temperature set point of 35°C is chosen for SH, and the free-cooling temperature set point is 18°C for SC distribution.

For concept C (4-pipe with DHW circulation loop), the temperature in the circuit for SH and SC follows a regular heating curve, with the same switching methodology to SC (18°C) as described before. The DHW circulation loop temperature is fixed at 60°C, controlled by a bypass valve on top off the riser pipe with a maximum temperature drop of 5°C to prevent the growth of *legionella bacteria*.

2.4. *Simulation-based Evaluation Framework*

2.4.1. *Mathematical Description of General Modelling*

A dynamic simulation environment is built in Python, based on the Matlab models of Van Riet [34] and extensively described in Jacobs et al. [15]. The transient thermal behaviour of all components in a CHCS are represented by first order, ordinary, linear, and non-homogeneous differential equations. The general equation is as follows:

$$\frac{dy(t)}{dt} = -a(t)y(t) + b(t) \quad (1)$$

with time, t, the independent variable and y the integrand. However, all differential equations are implemented as a explicit solution, according to a zero-order hold [34]. Therefore, $a(t)$ and $b(t)$ are constant within each time step (Δt). Notably, the simulation is executed with a Δt of 10 seconds to capture the effects of concept choices on DHW (and indoor) thermal comfort.

2.4.2. *Model: Thermal Energy Storage*

The stratified storage tank model is based on Type 60 of TRNSYS [38] and is described in [34, 15]. In general, the storage tanks are simulated as a partial differential equation in temperature and along the height [39]. It assumes a number of homogeneous volume layers with a uniform temperature to simulate the heat transport and stratification inside thermal storages. In this respect, the captured thermodynamics include conduction, advection, heat losses to surrounding, and heat gains from a potential internal coil heat exchanger. A temperature-inverse algorithm was added to account for the effect of temperature on the density of water.

In case of a TES for technical water, the inlet and outlet are at the top and bottom of the storage tank and water flows in both ways (representing the charging and discharging of the tank). In case of DHW storages, cold domestic water of 10°C enters the tank at the bottom during a DHW demand and the DHW exists the tank at the top. The circulation loop for the 4-pipe system is connected at 1/3 of height.

2.4.3. Model: Booster Heat Pump

The GHP, high-temperature GHP and decentralised BHP are all grey-box models, based on data regarding power consumption and heat generation at various source and sink temperatures. In this respect, the GHP is based on *Viesmann's Vitocall 300*, the high-temperature GHP on the *Enevator Aqua Booster WWHB of A.O.Smith*, and the BHP are based on *Alpha Innotec WWB21 of Nathan Systems*. This section section describes the BHP model in detail.

The BHP model is similar to the Geothermal Heat Pump (GHP) model of [34], with the difference that here the evaporator's outgoing temperature ($T_{eva;out}$) is also modelled. The condenser and evaporator are considered to be two separate lumped capacities where the condenser temperature (T_{con}) equals its outgoing flow temperature ($T_{con;out}$) and similar for the evaporator: "$T_{eva} = T_{eva;out}$". The model relies on mass and energy flows as its basis, outlined by Equations 2 and 3:

$$C_{con}^{BHP}\left(\frac{dT_{con;out}}{dt}\right) = \dot{Q}_{con}^{BHP} - UA_{con} \cdot (T_{con;out} - T_z) + c_p \cdot \dot{m}_{con} \cdot (T_{con;in} - T_{con;out}) \quad (2)$$

$$C_{eva}^{BHP}\left(\frac{dT_{eva;out}}{dt}\right) = -\dot{Q}_{eva}^{BHP} - UA_{eva} \cdot (T_{eva;out} - T_z) + c_p \cdot \dot{m}_{eva} \cdot (T_{eva;in} - T_{eva;out}) \quad (3)$$

with subscripts *con* and *eva* referring to condenser's and evaporator's side, respectively, now denoted as X: C_X^{BHP} the thermal capacities [J/K]; UA_X the overall heat transfer coefficient [W/K] to the surroundings (at 20°C); $\dot{m}_X$ the flow rate [kg/s], $T_{x;in}$ and $T_{x;out}$ the in- and outgoing temperatures [°C], respectively; and c_p the specific heat capacity of flow medium, which is for water 4187 J/KgK. Lastly, $\dot{Q}_{con}^{BHP}$ is the generated heating power of the condenser [W], and $\dot{Q}_{eva}^{BHP}$ is the extracted heat at evaporator side [W].

The $\dot{Q}_{con}^{BHP}$ and the electrical power consumption ($\dot{A}_{el}^{BHP}$) can be determined using the generalised polynomial of Equation 4:

Table 1: Polynomial parameters used in BHP model fitted on data of Alpha Innotec WWB21. In Equation 4, $\dot{Y}^{BHP}$ represents $\dot{Q}_{con}^{BHP}$ or $\dot{A}_{el}^{BHP}$, and the coefficients are accordingly.

	$\dot{Q}_{con}^{BHP}$	$\dot{A}_{el}^{BHP}$
p_0	2891,3	593
p_1	-3268,7	-556,7
p_2	-4201,9	-951,5
p_3	4383,3	884,8
p_4	539,5	10,8
p_5	1500,4	380
p_6	-438,8	-10
p_7	-1398	-348,6
R^2 value	0,9996	0,9979

$$\frac{\dot{Y}^{BHP}}{\dot{Q}_{con,nom}^{BHP}} = p_0 + p_1 \cdot T^{src} + p_2 \cdot T^{snk} + p_3 \cdot T^{src} \cdot T_{snk} + p_4 \cdot T^{src^2} + p_5 \cdot T^{snk^2} + p_6 \cdot T^{snk} \cdot T^{src^2} + p_7 \cdot T^{src} \cdot T^{snk^2} \quad (4)$$

The respective coefficients (p_0, p_1, p_2, p_3, p_4, p_5, p_6, p_7) of this polynomial are listed in Table 1 for $\dot{Y}^{BHP}$ representing either $\dot{Q}_{con}^{BHP}$ or $\dot{A}_{el}^{BHP}$. The parameter estimation was performed based on data from the *Alpha Innotec WWB21 from Nathan Systems* using a 'fit nonlinear regression model', resulting in high R²-values (0.9996 and 0.9979, respectively). In the context of the model, T^{src} and T^{snk} represent $T_{eva;in}$ and T_{con} in Kelvin, respectively, normalised by dividing each temperature by 273.

These coefficients and the fitted model enable the prediction of heat output ($\dot{Q}_{con}^{BHP}$) and electrical power input ($\dot{A}_{el}^{BHP}$) relative to the nominal heating power ($\dot{Q}_{con,nom}^{BHP}$) based on the given input temperatures (T^{src} and T^{snk}). The high R^2-values indicate the effectiveness and accuracy of the fitted polynomial model for this application.

2.4.4. Other Simulation Models

Each dwelling is simulated as a thermal zone with three temperature nodes, namely emitter surface temperature, indoor air temperature and indoor wall surface temperature. All three have an individual thermal capacity and heat exchange resistance. The model takes account of transmission losses, ventilation losses, internal heat gains and solar heat gains. For a detailed simulation of heat transmission the emitters are divided into nine segments, similar to the approach described in [15, 34].

The control signals of valves and pumps adjust the flow rate without depending on pressure models and hydraulic phenomena such as valve authority. In this respect, the mass flow between the nominal value and 10% of this value is guaranteed to be available. Time delays of control valves are taken into account with a time constant (τ) of 32s as in [34] and the mixing rule is applied for three-way valves and mixing points.

The time delay in the pipes is modelled by applying the plug-flow principle [40] and their thermal losses are characterised by an RC-model. For taking account of the required pumping energy to overcome pressure drops in the central piping network, the Darcy-Weisbach equation (5) is used.

$$\Delta p = f_D \cdot L \cdot \frac{\rho}{2} \cdot \frac{\overline{v}^2}{D_H} \tag{5}$$

Where Δp is the pressure drop [Pa], L the length of the distribution pipe [m], f_D the Darcy friction factor, calculated according to the Moody approximation [41], ρ the density of water, $\overline{v}$ the average flow velocity [m/s], and D_H the hydraulic diameter of the pipe [m].

The total power consumption of the central distribution pump, or two central pumps in case of the 4-pipe system, (E_{pump}) in [kWh] is calculated according to Equation 6.

$$E_{pump} = \dot{m}_{pipe} \cdot (\frac{\rho \cdot g \cdot H + \Delta p}{\rho \cdot \eta_{pump}} \cdot \Delta t) \cdot f_{conv} \tag{6}$$

Where g equals 9.81 m/s^2, H the pump head [m] (zero for closed loop circuits), η_{pump} the electric efficiency of the pump, f_{conv} the conversion factor from Joule to kWh, i.e. $\frac{1}{3.6 \times 10^6}$, and the rest as before. The η_{pump} is set to 70% to also account for the pumping cost of other smaller pumps in the system.

2.5. Post-Processing

2.5.1. Key Performance Indicators

The calculation of the holistic KPI score involves the utilization of four KPIs. These encompass one financial KPI and three KPIs dedicated to evaluating thermal comfort. The three comfort-oriented KPIs comprise two KPIs related to indoor thermal comfort and one addressing DHW comfort.

Regarding indoor thermal comfort, the daily average number of degree hours that the indoor operative temperature (T_{op}) deviates from its set point ($T_{op;SP}$) is calculated for each dwelling, with a tolerance of e_{tol} [°C]. Specifically, this entails the quantification of room temperature lack (RTL) [Kh/day] during heating conditions and room temperature excess (RTE) [Kh/day] during cooling conditions [34]. The RTE and RTL are presented as the average across all dwellings, delineated by Equation 7, in which n denotes the number of dwellings, and the rest as before:

$$\begin{aligned} RTL &= \frac{\sum_{i=1}^{n}(\int_{t_1}^{t_2}(T_{op;SP_i} - (T_{op_i} + e_{tol}))dt)}{n} \\ RTE &= \frac{\sum_{i=1}^{n}(\int_{t_1}^{t_2}((T_{op_i} - e_{tol}) - T_{op;SP_i})dt)}{n} \end{aligned} \tag{7}$$

The DHW comfort is assessed through the KPI denoted as relative duration of lacking DHW temperature ($t_{DHW;dc}$) [%], a KPI introduced in [15]. This metric quantifies the duration of DHW consumption with a DHW temperature below 40°C, expressed as a percentage relative to total tapping time. Figure 5 provides as illustrative example, where the red temperature line represents the available temperature in the dwellings for DHW consumption, and the blue line depicts the total tapping time of all dwellings (time B).

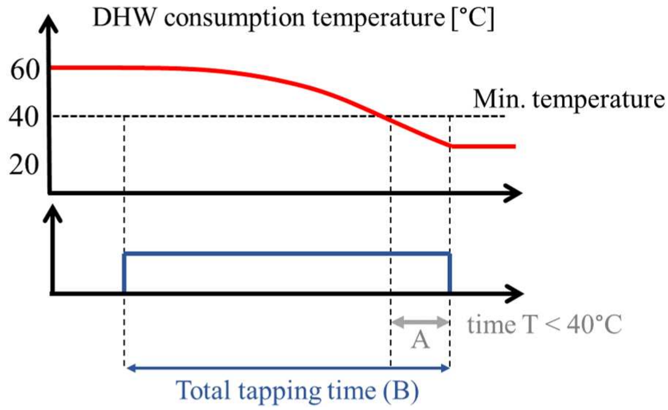

Figure 5: Used DHW discomfort Key Performance Indicator (KPI). This KPI ($t_{DHW;dc}$) is calculated as A/B, where B is the total DHW tapping time of all end-users and A is the total time at which the DHW temperature is below 40°C.

In this context, DHW discomfort is defined when the available temperature is below 40°C, corresponding to time A. Consequently, the relative duration of DHW discomfort is A/B (%). A lower percentage indicates a reduced average duration of discomfort experienced by end-users. It is noteworthy that the DHW flow rate assumes an ideal mixing valve at the tapping points, regulating the mass flows to achieve a consumption temperature of 40°C.

The financial KPI is the Levelised Cost of Energy ($LCOE$), expressed in €/kWh and calculated through Equation 8. This KPI is the ratio between the sum of Capital Expenditures ($CAPEX$) and the Operative Expenses ($OPEX$), and the total energy consumed by end-users [24, 42]. The total energy consumed is the absolute sum of space heating, space cooling and DHW consumption. In this ratio, both the costs and energy consumption are the discounted sum over a specified period, following the advise of [28] to employ Net Present Value in comparative analyses of CHCS.

$$LCOE = \frac{CAPEX + \Sigma_{t=1}^{N} OPEX \ \frac{1}{(1+r)^t}}{\Sigma_{t=1}^{N} Q_{used} \ \frac{1}{(1+r)^t}} \tag{8}$$

Where $CAPEX$ is the investment cost [€], including only the differences between the concepts (i.e. neglecting the costs of underfloor heating or the costs for the BTES field), $OPEX$ is the annual operating expenditure associated with energy use related to gas and electricity [€], N the considered time frame of 25 years, t the time [years], and Q_{used} the total useful energy for all end-users [kWh]. All assumptions for these calculations are presented in Table 2 with their respective references.

The diverse dimensions and value ranges of the considered KPIs pose a challenge in comparing overall performances for decision-making purposes. Although Pareto-front plots are currently utilised for comparisons, this approach is inherently subjective and prone to different interpretations among individuals. Addressing this challenge necessitates the establishment of a holistic KPI score (KPI^*) that translates the diverse KPIs or criteria into a unified value for objective evaluation.

Table 2: Financial data for LCOE calculations. The investment costs are fitted on available data from given references.

	Investment costs [€]	Ref.
Central GHP	€$642/kW$	[43]
HT-HP (x kW)	$(x > 0) \cdot (1.1553x^2 + 130.88x + 18399)$	A.O. Smith data
Storage tank (y litres)	$254.35 \cdot y^{0.3585}$	[44]
DHW BHP	€$1500/kW$	Market prices
Distribution pipes	$L \cdot (-0.0245D_H^2 + 6.3787D_H + 154.99)$	[45]
Maintenance cost	2% of investment cost	[46]
Discount rate	6%	[46]

2.5.2. Holistic KPI Score: KPI^*

Each of the four KPIs within a given experiment (Z, i, j, k, l)—with Z representing the concepts under evaluation, i corresponding to the occupancy profile, and j indicating the building variations, k the considered tariff structures, and l the weather profiles—is divided by its respective median value within experiment (i, j, k, l) for normalised and dimensionless KPIs. The medians within experiment (i, j, k, l) are solely based on the respective KPIs of CHCS Z in that specific experiment. To give an example, when calculating the median of RTL for experiment (i, j, k, l), the RTL values of concepts Z within that experiment are utilised. The advantage of using the median in the normalisation method is that it preserves the relative differences in performance between distinct concepts.

Based on this normalisation methodology, the financial KPI is translated into an aggregated cost KPI ($KPI_{costs}(Z, i, j, k, l)$) and the three thermal comfort KPIs into an aggregated comfort KPI ($KPI_{comfort}(Z, i, j, k, l)$) per experiment (i, j, k, l), through a weighted sum. Equation 9 illustrates this for $KPI_{costs}(Z, i, j, k, l)$ consisting of only one KPI, i.e. $LCOE$. The median of the considered CHCS's $LCOE$ for boundary conditions i, j, k, l is denoted as $\mu_{LCOE}(i, j, k, l)$.

$$KPI_{costs}(Z, i, j, k, l) = \frac{LCOE(Z, i, j, k, l)}{\mu_{LCOE}(i, j, k, l)} \tag{9}$$

Analogous to $KPI_{costs}(Z, i, j, k, l)$, the $KPI_{comfort}(Z, i, j, k, l)$ is calculated according to Equation 10. Here, for every experiment (i, j, k, l), the three normalised comfort-based KPIs are summed using a weighted sum, with weights α_i for DHW comfort, β_i for SH comfort and γ_i for SC comfort. The values for these weighting factors are determined based on the relative share of DHW demand, SH demand and SC demand for the different occupant profiles i.

$$\begin{aligned} KPI_{comfort}(Z, i, j, k, l) = \alpha_i \cdot \frac{t_{DHW;dc}(Z, i, j, k, l)}{\mu_{t_{DHW;dc}}(i, j, k, l)} &+ \\ \beta_i \cdot \frac{RTL(Z, i, j, k, l)}{\mu_{RTL}(i, j, k, l)} &+ \\ \gamma_i \cdot \frac{RTE(Z, i, j, k, l)}{\mu_{RTE}(i, j, k, l)} & \end{aligned} \tag{10}$$

Finally, the aggregated KPI scores for the multi-objective criteria, i.e. costs and thermal comfort in this manuscript, are merged into a holistic KPI score (KPI^*), with respect to the input values representing the end-user preferences regarding conflicting objectives (Equation 11).

$$\begin{aligned} KPI^*(Z, i, j, k, l) = -\,(f_{costs} \cdot KPI_{costs}(Z, i, j, k, l) &+ \\ (1 - f_{costs}) \cdot KPI_{comfort}(Z, i, j, k, l)) & \end{aligned} \tag{11}$$

Where f_{costs} is the importance given to minimising the costs $\in [0,\ 1]$, and the other variables as before. KPI^* is always negative with 0 the best value.

The proposed methodology exhibits certain limitations. Firstly, utilising the median as a normalisation strategy preserves relative performance differences between distinct concepts, transforming the KPI^* into a relative comparison among concepts. This implies that the KPI^* of a specific concept within experiment (i, j, k, l) is dependent on which other concepts Z are included in the comparative analysis. Consequently, the methodology cannot serve as a general scoring technique unless all other concepts undergo the same comparative analysis.

Additionally, the computational complexity associated with our methodology, particularly in executing simulations, may present practical challenges for widespread adoption, especially in resource-constrained settings. Despite these limitations, our methodology represents a notable advancement in CHCS evaluation and selection, providing valuable insights for decision-makers.

3. Results and Discussion

To demonstrate and validate the proposed evaluation methodology, a comparative analysis of three innovative central change-over systems: A, B and C (see Section 2.3.1 for details) is conducted using a detailed case study. In this respect, four different occupancy profiles ($i = 4$) and five different apartment building sizes ($j = 5$) are considered to generate tailored recommendations. The same tariff structure and weather profile are used across all analyses ($k = l = 1$), with the case study conducted in Flanders, Belgium. More details on the case-specific inputs for the design of experiments are provided in Section 3.1, with the analysis in Section 3.2. The discussion further extends the results by interpolating to other building sizes and occupancy profiles, and examines the robustness of the KPI^{*} in generating recommendations.

3.1. Design of Experiments: Case-Specific Inputs

The scheme in Figure 6 illustrates the demonstration of the novel evaluation methodology applied to generate recommendations for three central change-over systems referred to as A, B, and C. The design of experiments is configured as ($Z = 3, i = 4, j = 5, k = 1, l = 1$), facilitating a two-dimensional analysis where family types are represented on the x-axis, and the number of dwellings in the apartment building on the y-axis.

The variation in number of dwellings, ranging from 8 to 50, is important for evaluating central change-over systems because the distribution network needs to switch between several temperatures. This is expected to be more cost and time intensive in larger apartment buildings. Additionally, understanding the impact of different family types, each characterised by distinct energy consumption profiles, is key for evaluating CHCS performance and tailoring recommendations based on specific occupancy profiles. Based on data available from [47, 48], four occupant behaviour profiles have been selected to represent the population in Flanders:

I) **Retirement profile** (21% of Flanders' population): Represents an energy consumption profile of two retired people often at home. Their DHW demands are typically lower than other profiles, but SH demands are higher due to an higher indoor temperature set point ($T_{op;SP}$) of 23°C during the day.

II) **Working 2-person families** (25%): Characterised by moderate demands across SH, DHW, and possibly space cooling (SC), influenced by lifestyle and work schedules. Each dwelling has three tapping points and a daytime $T_{op;SP}$ of 21°C.

III) **Working 4-person families with school-going children** (41% combined with family type IV): Similar to family type II but with two school-going children, resulting in higher SH and DHW demands and potential variability in SC needs.

IV) **Luxurious 4-person families with school-going children** (41% combined with family type III): Represents 4-person households with increased energy demands, particularly for DHW, due to higher standards including a bath, rain shower and four tapping points.

For all family types, $T_{op;SP}$ is reduced by 2°C at night during heating conditions. During cooling conditions, $T_{op;SP}$ adapts to the outdoor temperature, with a temperature difference set at 5°C and a minimum $T_{op;SP}$ of 25°C. For calculations involving RTL and RTE, the tolerance (e_{tol}) is set at 0.5°C. Figure 7 shows the differences in energy consumption profile between these four family types for **(a)** the cumulative DHW demand and **(b)** the internal heat gains of a representative household.

With respect to the sizing of the decentralised storage tanks, the 'Power-Storage'-method of [36] is used. For concept A, the heating power is 3.5 kW as described in Section 2.3.2, while for concept B, the assumed heating power is 2kW by default, but reaching 2.5kW for luxury family types due to an increased DHW consumption. Based on these assumptions for heating power, the storage tanks in concept A are sized at 140 litres, 150 litres, 160 litres and 280 litres for family types I, II, III, and IV, respectively. For concept B, the corresponding tank sizes are 155 litres, 166 litres, 185 litres and 297 litres, respectively.

The required input parameters for building characteristics, not related to family type or number of dwelling, are highlighted next. The overall U-value of the walls is 0.24 W/m²K and all windows are HR++ types, as required for newly built dwellings in Flanders [49]. These well-insulating windows have a U-value of 1.1 W/m²K and a solar radiance transmission factor of 0.6 (g-factor). The floor areas of different dwelling configurations range between 88 m² and 104 m² and the window areas are 21% of the respective floor area, facing different solar orientations. Each dwelling has ventilation type D (mechanical, balanced ventilation) with a heat recuperation efficiency of 80%. However, when the outdoor temperature exceeds 16°C, the heat recuperation is bypassed. During SC mode, the ventilation rate increases when the indoor temperature surpasses both 25.5°C and the current outdoor temperature. This increase corresponds to an additional hourly refreshment of the indoor air volume.

For the tariff structure, the Belgian Endex101 contract of 2023 is considered in the analyses and shown in Figure 8. This price setting is typically applied in Belgian residential buildings with a variable contract. Given that the considered CHCS for demonstration are only equipped with power-to-heat units, the tariff structure for gas usage has been excluded.

The weather file used in the demonstration represents the average climate conditions in Belgium spanning from 2001 to 2020 and was generated by Buildwise as part of the IEA EBC Annex 80 project [50]. Based on this weather file, three representative months are selected to capture the year-round performance of the to be evaluated central change-over systems. Specifically, January was selected to represent winter conditions, July to represent summer conditions, and September 15 to October 15 to emulate spring/autumn conditions.

The distribution of these representative months aligns with the example depicted in Figure 2. This means that the simulation results obtained for January also stand for February, November and December. Similarly, the results for July apply to May, June and August. The remaining four months of the year are represented by the September 15 to October 15 period.

Based on preliminary simulations, Table 3 provides an overview of the absolute and relative shares of SH, SC, and DHW demand for each family type inhabiting the apartment buildings. The relative shares are used to define the weighting factors in Equation 10 for calculating $KPI_{comfort}(Z, i, j, k, l)$. The annual energy usages per square metres range from 53.1 kWh/m²a (family type II) to 67.6 kWh/m²a (family type IV), potentially qualifying these buildings as near-zero energy buildings according to European standards. However, defining buildings solely based on this energy metric is challenging due to various factors and mixed usage of terminology in this context [51].

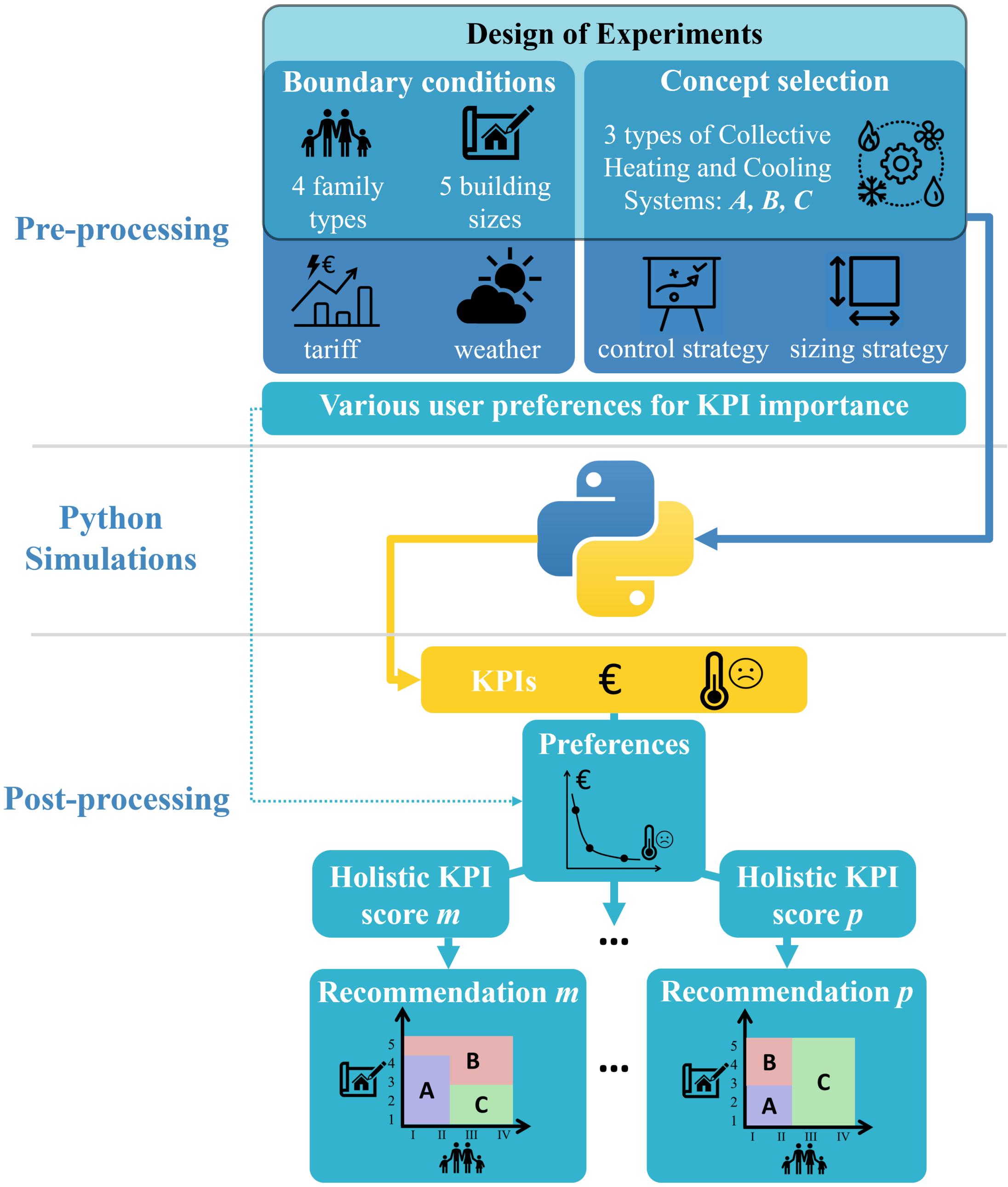

Figure 6: Schematic overview of the design of experiments, considering 4 different family types, 5 building sizes, 1 tariff structure and 1 weather profile to generate recommendations for 3 distinct CHCS concepts (A, B, C). The optimal CHCS is determined for each boundary condition, taking into account varying preferences for thermal comfort and costs.

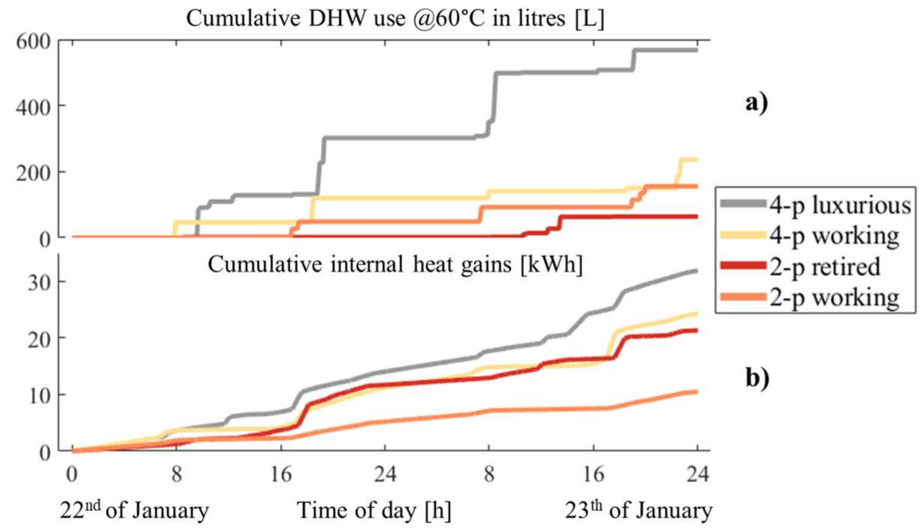

Figure 7: Figure **(b)** shows an example of the cumulative DHW profile and **(c)** of the cumulative internal heat gain profile for the four different family types. The profiles are given for the 22nd and 23th of January and are different for all dwellings.

Table 3: Absolute and relative shares of DHW demand, SH demand and SC demand for different occupancy profiles i. The relative shares are used for defining the weighting factors ($\alpha_i, \beta_i, \gamma_i$) in Equation 10 for calculating $KPI_{comfort}(Z, i, j, k, l)$.

	Occupancy profile i			
	1	**2**	**3**	**4**
	Retired	**working 2-p**	**working 4-p**	**luxurious 4-p**
DHW $[kWh/m^2a]$	16.1	17.8	26.1	35.7
SH $[kWh/m^2a]$	33.4	26.5	21.5	20.8
SC $[kWh/m^2a]$	10	8.8	10.9	11.1
α_i	0.29	0.35	0.47	0.55
β_i	0.58	0.52	0.39	0.32
γ_i	0.13	0.13	0.14	0.13

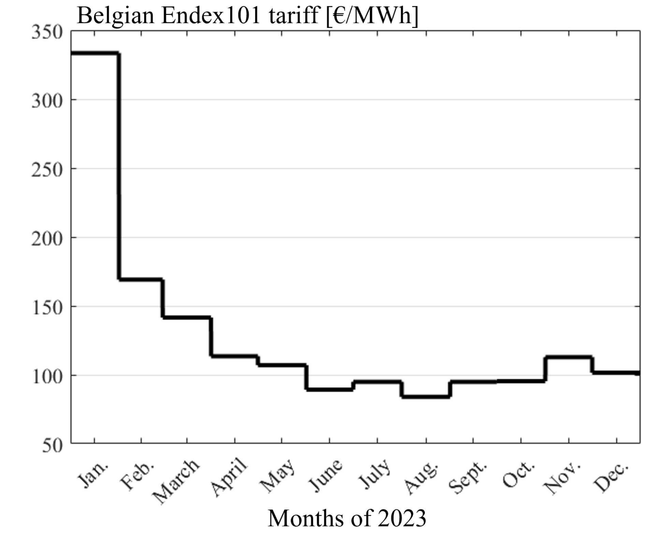

Figure 8: This figure shows the used electricity price signal [€/MWh], following the Endex101 price setting of 2023 in Belgium.

3.2. Comparative Analysis

Figure 9 visualises recommendations corresponding to four distinct occupants' preferences characterised by varying values of f_{costs} (0, 0.6, 0.9 and 1). The general trend indicates that when the importance assigned to comfort surpasses that of costs, the 4-pipe system (concept C) consistently emerges as the recommended choice across all investigated scenarios, particularly for $f_{costs} \in [0, 0.57]$. This aligns with initial expectations, as the expensive concept C provides outstanding comfort. However, starting at $f_{costs} = 0.6$, concept B begins to emerge as an interesting alternative. In the first place for luxurious family types, and subsequently for other family types as well. When cost reduction takes full importance over thermal comfort, concept B is recommended for all building sizes and occupancy profiles considered in this research.

Figure 10 provides a detailed breakdown of the four KPIs and the two aggregated KPI values. Despite concept C consistently exhibiting the highest $LCOE$, it is recommended when comfort is prioritised ($f_{costs} \leq 0.6$). This recommendation stems from I) minimal DHW discomfort ($t_{DHW;dc}$, which is between 0 and 0.02, and II) both RTL and RTE of concept C consistently aligning with or slightly surpassing the performance of the other concepts. Therefore, the $KPI_{comfort}(Z, i, j, 1, 1)$ for $Z = C$ values ranges between only 0.45 and 0.78. In contrast, for $Z = A$ this ranges between 1.18 and 1.85, and for $Z = B$ the range is between 1.17 and 13.5, respectively.

Similarly, concept B consistently achieves the lowest $LCOE$ for all investigated boundary conditions, making it the preferred choice when reducing costs is paramount. However, its $t_{DHW;dc}$ is always relatively high, compared to the other systems, which means that the BHP have not sufficient heating power or storage volume compared to other systems.

The transition from the 4-pipe system to concept B as the preferred choice does not occur abruptly with an increase in f_{costs}. Instead, an intermediate phase is observed where the optimal concept is contingent on the occupancy profile and/or building size. For instance, even concept A is recommended in some situations. This is true for f_{costs} within $[0.79, 0.97]$, and particularly in small apartment buildings with minimised DHW consumption throughout the day. This consumption pattern is typical for working families, i.e. profiles II and III.

Two main factors contribute to concept A's recommendations in that particular case. Firstly, the two-sensor control in concept A is optimal for a uniform DHW consumption pattern across the entire building. This uniform pattern particularly exists for working families, where DHW consumption is concentrated around the morning and evening when people are home. This facilitates the grouped charging strategy, ensuring simultaneously charging of all storage tanks. Moreover, the minimal DHW consumption throughout a significant part of the day provides ample time for the storage tanks to recharge.

Secondly, the $LCOE$ of concept A in small apartment buildings is low. However, as building size increases, concept A's $LCOE$ converges with that of concept C, reaching a comparable price in larger dwellings. This is because the delivered SC to end-users is relatively lower for concept A than for concept C, which is also reflected in the 3 times higher SC discomfort.

Starting at $f_{costs} = 0.98$, concept B emerges as the preferred concept across all experiments. However, within the range $f_{costs} \in \,]0.57, 0.98[$ the transition is not uniform across all considered boundary conditions. The designation of concept B as recommended CHCS initially occurs for luxurious occupancy profiles, followed by retired profiles from $f_{costs} = 0.8$, and finally for occupancy profiles II and III. This transition is influenced by the relative importance assigned to comfort in the calculation of KPI^*. As illustrated in Figure 10, the $t_{DHW;dc}$ for concept B is consistently higher than for concepts A and C. However, in the case of luxurious occupancy profiles, concept A also exhibits a higher $t_{DHW;dc}$ compared to other occupancy profiles. This results in a higher median ($\mu_{t_{DHW;dc}}(i, j, 1, 1)$) for this specific occupancy profile, diminishing the impact of the even poorer $t_{DHW;dc}$ of concept B in the final calculation of KPI^*. Moreover, the relative share of DHW, accounting for 55% of the total energy consumption for occupancy profile IV, further accentuates the impact of DHW comfort. This results in concept B being recommended earlier due to its superior $LCOE$ compared to its poorer $KPI_{comfort}(Z, i, j, 1, 1)$.

As previously mentioned, the KPI^* of a concept is dependent on the evaluation of the other concepts in that experiment, i.e. boundary conditions. Consequently, when concept A, with a 2SC, encountered challenges in managing the non-uniform DHW pattern of a luxurious family type, the DHW discomfort resulting from concept B becomes less pronounced. A similar effect is observed for the retired occupancy profile.

3.3. Interpolation of Main Results

The preceding section provided a comprehensive analysis and discussion of the results for the considered family types and building sizes. However, in reality, a broader range of consumption patterns and building sizes exists, necessitating the interpolation of results to generate recommendations across this

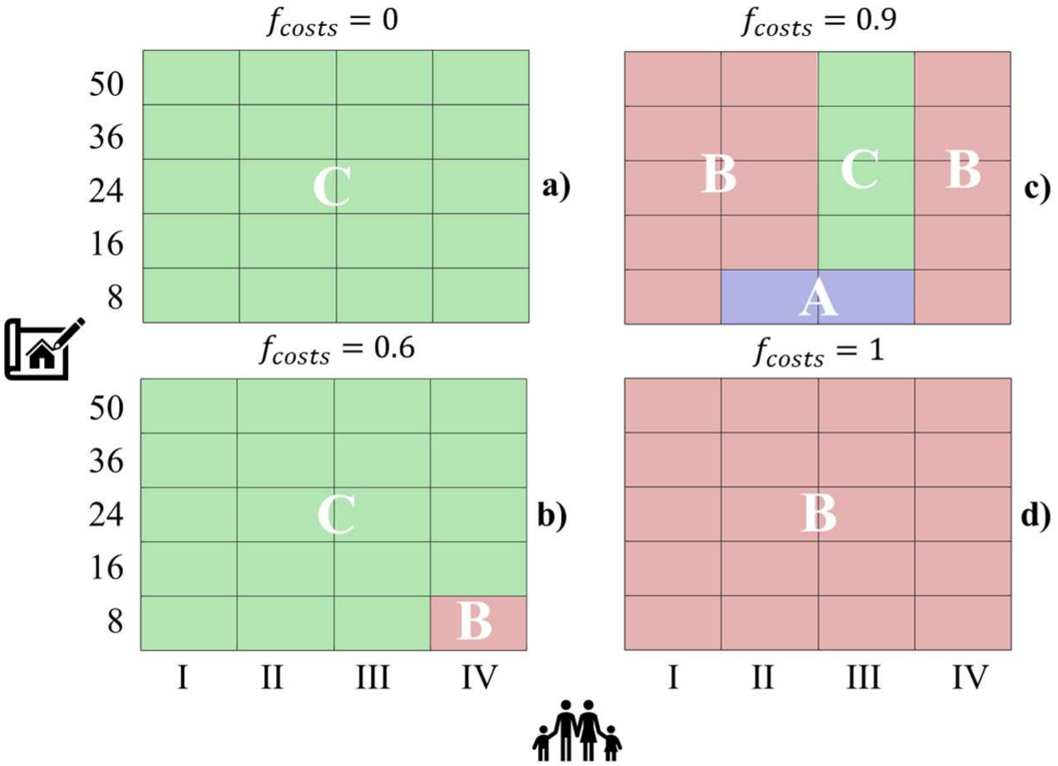

Figure 9: Results for f_{costs} equal to **(a)** 0, **(b)** 0.6, **(c)** 0.9 and **(d)** 1. The x-axis represents the four different family types: I) retired people, II) working 2-person, III) working 4-person, and IV) luxurious 4-person. The y-axis is the number of dwellings.

entire range. To achieve this, an essential step involves characterising the occupancy profiles for effective interpolation. Note that this research focuses on interpolation for building size and occupancy profiles, with potential for future work to expand the results through extrapolation.

As observed in Table 3 from Section 2.5.2, the share of SC is always circa 13%. Consequently, characterising different family types can be accomplished based on the ratio of their SH share to DHW share in the total yearly energy consumption. Figure 11 provides an example of the characterisation for family type I. However, it should be noted that characteristics such as number of daily change-overs in distribution temperature due to demanded temperature levels or usual moments of DHW consumption is not reflected in this metric, while it also affects the systems' performance.

Figure 12 displays the interpolated results for $f_{costs} = 0.8$ and $f_{costs} = 0.9$, using linear interpolation. These graphs affirm the findings of the previous section, indicating that initially concept C is preferred, but with an increasing f_{costs} the decentralised BHPs become more prominent.

Additionally, it should be noted that these recommendations are tailored for newly built apartment buildings. In the context of renovation projects, the installation of 4-pipe systems might pose challenges due to space constraints within existing shafts, making them prohibitively costly. In such cases, the 2-pipe with decentralised DHW storages might emerge as a viable alternative, offering a KPI^* relatively closely comparable to the 4-pipe system. This alternative could therefore be preferred more often, especially when the primary focus is on minimising expenses.

3.4. Relative Differences in KPI^*

In the previous analyses, the focus was primarily on identifying the best-performing systems. However, in some cases, the difference in KPI^* between different concepts can be minimal. Therefore, a 3-D graph can be employed to reveal those points where KPI^* are coming really close.

Figure 13 shows the KPI^* for each concept when f_{costs} is set to 0.1 and 0.9. When $f_{costs} = 0.1$, the KPI^* of concept C is substantially lower than that of the other concepts. Concept A's KPI^* ranges between 60% and 199% higher values, while concept B's KPI^* is even higher (up to 14.5 times higher). This suggests that concept C is the clear preferred choice when primary focus is on comfort. However, as f_{costs} increases to 0.9, the overall shape of all three KPI^*-planes remains relatively constant, but moves along the Z-axis. The KPI^*-plane for concept C drops to around -1, while the plane for concept B approaches -0.8. This indicates that, as cost considerations become more significant, the performance of concept B becomes more competitive relative to concepts A and C. Only around a ratio of 1 between DHW demand and SH demand, concept C is not the best option, and concepts A and C are consistently very close to each other, with differences between 4% and 15%.

		$LCOE$ (€)	$t_{DHW;dc}$ (%)	RTL (Kh)	RTE (Kh)	KPI costs	KPI comfort	$LCOE$ (€)	$t_{DHW;dc}$ (%)	RTL (Kh)	RTE (Kh)	KPI costs	KPI comfort
	A	0,36	0,32	0,81	5,57	1,00	1,31	0,38	0,37	0,48	4,33	1,00	1,26
50	***B***	0,23	1,67	0,77	1,63	0,64	2,19	0,25	1,57	0,40	1,45	0,66	2,06
	C	0,36	0,00	0,90	1,60	1,01	0,78	0,38	0,02	0,52	1,45	1,01	0,72
	Median	0,36	0,32	0,81	1,63			0,38	0,37	0,48	1,45		
	A	0,39	0,36	0,53	4,73	1,00	1,85	0,41	0,35	0,22	3,56	1,00	1,66
36	***B***	0,25	1,88	0,47	0,62	0,65	2,13	0,27	1,63	0,20	0,59	0,66	2,22
	C	0,40	0,00	0,57	0,60	1,02	0,75	0,42	0,00	0,27	0,58	1,03	0,77
	Median	0,39	0,36	0,53	0,62			0,41	0,35	0,22	0,59		
	A	0,38	0,34	0,58	3,97	1,00	1,76	0,40	0,31	0,28	3,35	1,00	1,65
24	***B***	0,24	1,90	0,51	0,58	0,64	2,27	0,27	1,57	0,23	0,56	0,65	2,34
	C	0,39	0,00	0,62	0,57	1,03	0,76	0,42	0,00	0,32	0,54	1,03	0,72
	Median	0,38	0,34	0,58	0,58			0,40	0,31	0,28	0,56		
	A	0,36	0,28	0,61	2,50	1,00	1,45	0,38	0,28	0,31	1,96	1,00	1,36
16	***B***	0,24	1,59	0,52	0,56	0,65	2,28	0,26	1,29	0,27	0,52	0,68	2,20
	C	0,39	0,00	0,65	0,54	1,06	0,74	0,42	0,00	0,36	0,51	1,09	0,72
	Median	0,36	0,28	0,61	0,56			0,38	0,28	0,31	0,52		
	A	0,35	0,26	0,76	1,55	1,00	1,34	0,38	0,07	0,47	1,02	1,00	1,25
8	***B***	0,23	1,99	0,67	0,42	0,64	2,87	0,25	1,02	0,47	0,35	0,66	5,65
	C	0,40	0,00	0,79	0,38	1,13	0,72	0,43	0,00	0,50	0,33	1,16	0,68
	Median	0,35	0,26	0,76	0,42			0,38	0,07	0,47	0,35		
				Retired 2-person						**Working 2-person**			

		$LCOE$ (€)	$t_{DHW;dc}$ (%)	RTL (Kh)	RTE (Kh)	KPI costs	KPI comfort	$LCOE$ (€)	$t_{DHW;dc}$ (%)	RTL (Kh)	RTE (Kh)	KPI costs	KPI comfort
	A	0,38	0,13	0,67	6,87	1,04	1,68	0,35	2,04	0,24	7,51	1,00	1,21
50	***B***	0,24	2,14	0,22	2,73	0,65	8,10	0,23	3,14	0,22	2,86	0,67	1,27
	C	0,37	0,00	0,30	2,55	1,00	0,52	0,36	0,00	0,27	1,93	1,04	0,45
	Median	0,37	0,13	0,30	2,73			0,35	2,04	0,24	2,86		
	A	0,40	0,14	0,18	5,45	1,01	1,72	0,37	2,24	0,11	6,05	1,00	1,66
36	***B***	0,26	2,46	0,12	1,00	0,65	8,79	0,25	3,09	0,10	0,99	0,67	1,19
	C	0,40	0,00	0,15	0,81	1,00	0,50	0,38	0,00	0,14	0,89	1,03	0,53
	Median	0,40	0,14	0,15	1,00			0,37	2,24	0,11	0,99		
	A	0,39	0,16	0,16	4,83	1,00	1,76	0,35	2,29	0,12	4,44	1,00	1,48
24	***B***	0,25	2,33	0,11	0,76	0,64	7,14	0,24	3,08	0,12	0,95	0,69	1,19
	C	0,39	0,01	0,16	0,77	1,00	0,54	0,38	0,00	0,15	0,85	1,07	0,53
	Median	0,39	0,16	0,16	0,77			0,35	2,29	0,12	0,95		
	A	0,38	0,20	0,18	3,62	1,00	1,61	0,34	2,34	0,15	2,92	1,00	1,29
16	***B***	0,24	2,43	0,13	0,69	0,64	6,16	0,24	3,19	0,16	0,86	0,71	1,20
	C	0,39	0,00	0,19	0,69	1,04	0,55	0,38	0,00	0,20	0,77	1,13	0,53
	Median	0,38	0,20	0,18	0,69			0,34	2,34	0,16	0,86		
	A	0,37	0,08	0,26	1,84	1,00	1,40	0,33	2,52	0,25	1,32	1,00	1,18
8	***B***	0,24	2,26	0,21	0,48	0,63	13,50	0,23	3,35	0,24	0,53	0,71	1,17
	C	0,41	0,00	0,27	0,47	1,10	0,54	0,40	0,00	0,29	0,56	1,22	0,51
	Median	0,37	0,08	0,26	0,48			0,33	2,52	0,25	0,56		
				Working 4-person						**Luxurious 4-person**			

Figure 10: All KPIs, $KPI_{costs}(Z, i, j, 1, 1)$ and $KPI_{comfort}(Z, i, j, 1, 1)$ used for calculating KPI^*.

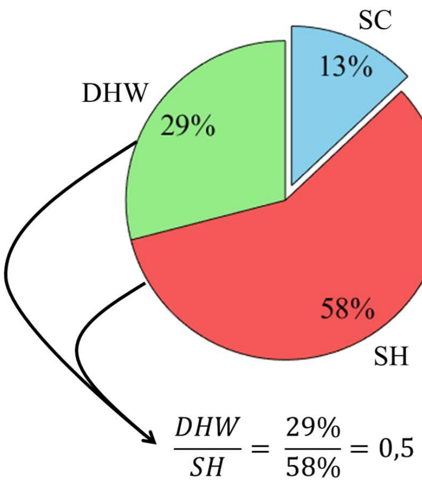

Figure 11: Example of characterization of family type I by considering the ratio of DHW demand to SH demand.

3.5. Discussion

The preceding analyses have demonstrated that concept B, despite its decentralised DHW production, consistently yields the highest levels of DHW discomfort. This resulted into a $KPI_{comfort}(Z, i, j, 1, 1)$ values for $Z = B$ reaching up to 13.5 in the case of occupancy profile III. The sizing methodology significantly influences this outcome. Consequently, for this respective occupancy type, the storage tank volumes have been increased from 185 litres to 420 litres. This adjustment aligns with the 'Power-Storage' method [36], wherein the basis for determining the storage volume is now the maximum of all peak cumulative DHW demands, as opposed to the previous reliance on the average peak.

It is noteworthy that the increased volume of 420 litres exceeds the typical market availability for storage tanks of BHPs. Despite this deviation from the norm, these increased volumes result in improved $KPI_{comfort}(Z, i, j, 1, 1)$ values for $Z = B$, ranging between 2.9 and 4.7. This suggests that the overarching conclusions remain valid, but the transition from concept C to concept B as the recommended concept with increasing f_{costs} would occur at a slightly accelerated pace. Additionally, the prominent downward peak in Figure 13 for family type III would be diminished to some extent. Similarly, increasing the heating power of BHPs would also improve the DHW comfort and thereby its evaluation.

In the current results, the DHW discomfort appears to have a significant influence on the $KPI_{comfort}(Z, i, j, 1, 1)$ values due to the weights defined based on the respective shares in total energy demand, as presented in Table 3. Adapting these weights yields different recommendations. However, the general conclusions persist, with another behaviour during the transition from $f_{costs} = 0$ to $f_{costs} = 1$. Only in extreme cases, such as neglecting DHW discomfort by setting α_i to 0, concept B becomes recommended for $f_{costs} \in [0, 1]$. Future work could focus on a comprehensive assessment of these influences on recommendations.

Similar conclusions apply to $KPI_{costs}(Z, i, j, 1, 1)$ and its im-

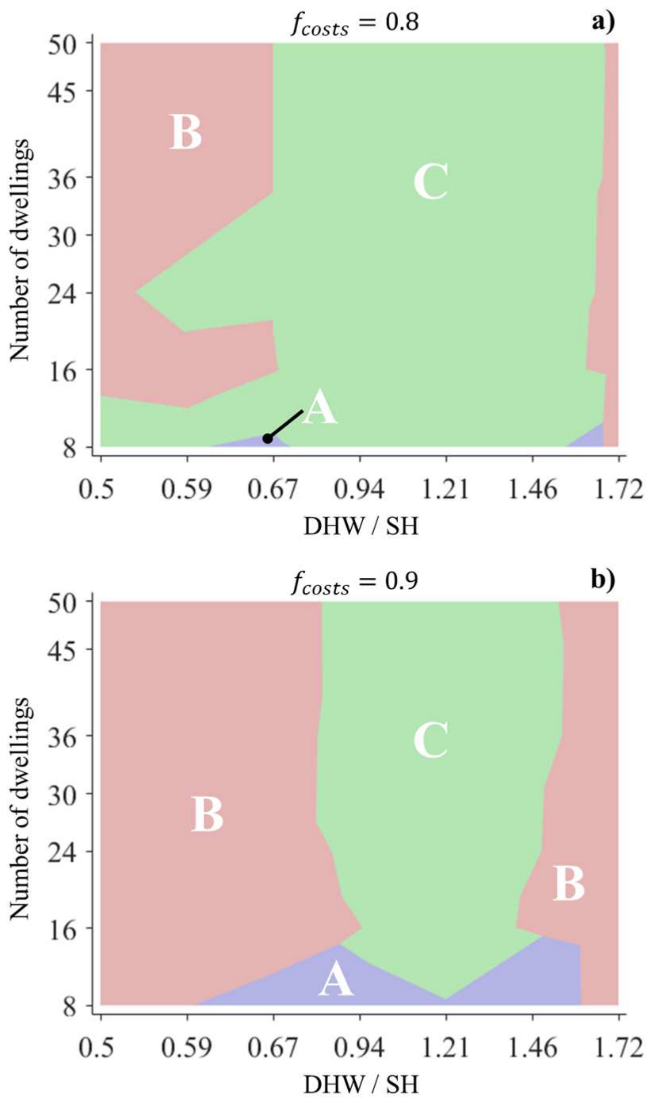

Figure 12: Recommendations for concept selection A, B and C, when preference is given to lower costs: **(a)** $f_{costs} = 0.8$, **(b)** $f_{costs} = 0.9$. The y-axis shows increasing number of dwellings and the x-axis represents family types by their share of SH over share of DHW in the total yearly energy demand (share of SC is always 13%).

pact on the recommendations. In this research, the $CAPEX$ considered only the differences between concepts A, B and C. Therefore, the cost of for example the central BTES field was not included because it would be similar for all concepts with the same boundary conditions i, j, k, l. However, to investigate the effects of these neglected costs, the $CAPEX$ was increased by €10k per dwelling for all concepts. As with different weights for $KPI_{comfort}(Z, i, j, 1, 1)$, the overall findings remain consistent but exhibit another pattern during the transition from $f_{costs} = 0$ to $f_{costs} = 1$. With the increased $CAPEX$, concept A and B are recommended concepts starting at higher f_{costs} of 0.67 instead of 0.6. This is primarily attributed to the relative nature of the KPI^* methodology.

The proposed evaluation framework and the KPI^* methodology prove valuable not only for generating recommendations regarding concept selection but also for assessing design decisions for specific concepts at an early stage. In this respect, different control strategies could be compared to ensure optimal performance under various situations while still considering the occupants' preferences. Furthermore, the design of experiment is expandable to include other boundary conditions for more comprehensive recommendations.

The novel methodology demonstrated its value for decision-makers selecting CHCS for apartment buildings. However, it is also applicable for policy makers aiming to promote or discourage specific heating and cooling concepts tailored to a range of boundary conditions. In this context, the considered KPIs should be expanded to include environmental KPIs such as CO_2 emissions. Consequently, the KPI^* would be a weighted sum of more aggregated KPIs.

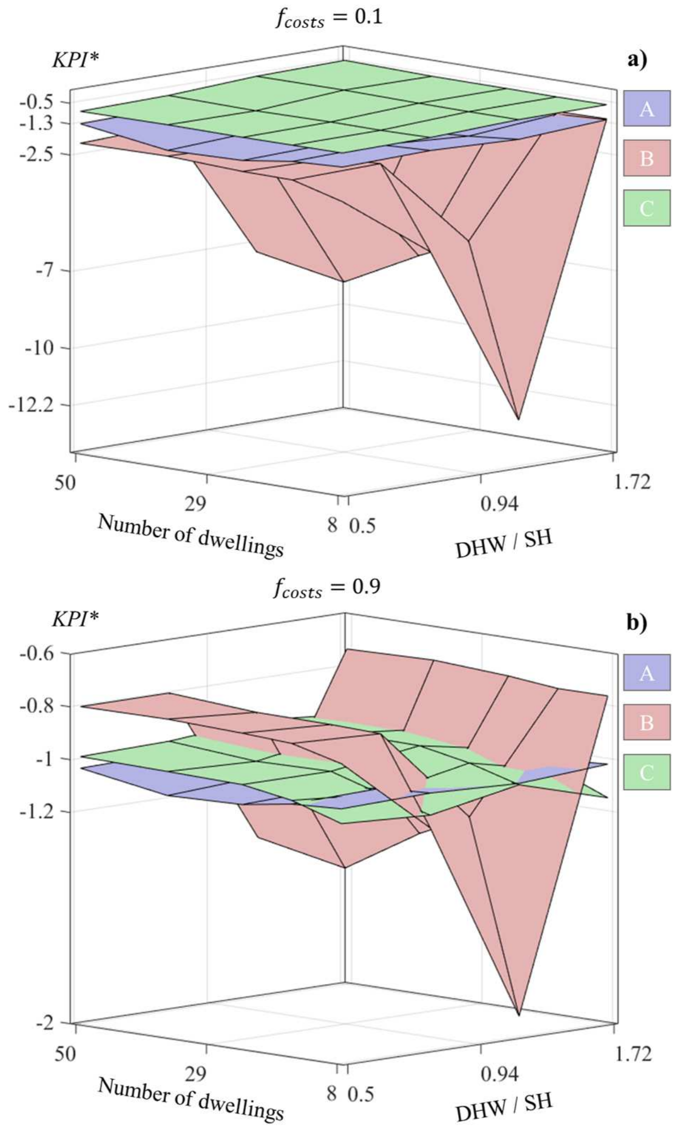

Figure 13: 3-Dimensional recommendations for concept selection A, B and C, when **(a)** $f_{costs} = 0.1$, and **(b)** $f_{costs} = 0.9$. The y-axis shows increasing number of dwellings and the x-axis represents family types by their share of SH over share of DHW in the total yearly energy demand (share of SC is always 13%).

4. Conclusion and Future Research

4.1. Conclusions

This paper presents a comprehensive evaluation methodology for multiple CHCS in diverse building scenarios. The methodology concerns a multi-objective decision-making approach for concept selection through a holistic KPI score, integrating occupants' preferences regarding (conflicting) criteria to generate recommendations for decision-makers.

The methodology is demonstrated by means of a comparative analysis of three state-of-the-art central change-over CHCS for various apartment building sizes and occupancy profiles. The conflicting KPIs considered are an aggregated thermal comfort indicator, encompassing DHW discomfort, RTL and RTE, and the aggregated expenses represented by normalised $LCOE$. The results highlight that 4-pipe systems are highly recommended for newly built apartment buildings when prioritising thermal comfort due to their low $t_{DHW;dc}$, despite higher $OPEX$. In contrast, decentralised BHPs outperform the 4-pipe and 2-pipe with decentralised DHW storages in terms of expenses for a broad range of building sizes and occupancy profiles. The 2-pipe system with decentralised DHW storages is preferred in smaller apartment buildings and for working family types, where DHW consumption patterns are concentrated, benefiting the 2SC.

In the broader context, the developed evaluation framework can serve as a valuable tool for testing and comparing sizing strategies or new control strategies, such as data-driven control techniques, under different environmental conditions (e.g. building characteristics, geographic locations, occupancy profiles, etc.). It also allows to investigate robustness of control strategies towards occupants' preferences and varying boundary conditions. Moreover, the methodology can be extended with other KPIs making it usable for policymakers. This would make policies tailored on specific boundary conditions possible. However, it is important to note that further research is required before full adaption of this methodology.

4.2. Future Research

Future research may expand the conclusions by incorporating additional concepts into the evaluation and exploring a broader range of boundary conditions, such as including different weather profiles and control strategies. This expansion aims to provide more general insights into concept selection. Moreover, the methodology could be used as an assessment framework for evaluating new control strategies under various boundary conditions and occupants' preferences, which is especially relevant for data-based control strategies.

Enhancement to the KPI^* representation could involve integrating more KPIs, such as CO_2-emission, primary energy use, and exergy efficiency, to broaden the criteria considered in the evaluation.

Addressing the challenge of setting the appropriate values for parameters like f_{costs} and the weights in $KPI_{comfort}(Z, i, j, k, l)$, future research could explore objective methods, such as the Shannon entropy technique [29]. Although this method may not fully incorporate occupants' preferences into the decision-making process anymore, it determines weights based on variations in different KPIs, offering a more objective weighting approach.

Moreover, there is potential to integrate the evaluation methodology into a holistic concept generator, automating the selection of the most optimal concept for a specific building characteristics. Additionally, control optimisation could benefit from in-the-loop data-driven techniques that consider occupants' preferences regarding conflicting KPIs.

Funding

This research was supported by a PhD fellowship of the Research Foundation Flanders (FWO) [1S08622N].

CRediT Authorship Contribution Statement

Stef Jacobs: Writing - original draft, Conceptualization, Validation, Investigation, Methodology, Visualization, Formal Analysis, Project administration. **Senne Van Minnebruggen:** Writing - review & editing, Validation. **Houssam Matbouli:** Writing - review & editing, Validation. **Sara Ghane:** Writing - review & editing. **Peter Hellinckx:** Writing - review & editing, Supervision, Conceptualization. **Ivan Verhaert:** Writing - review & editing, Supervision, Resources, Project administration, Conceptualization.

Declaration of Competing Interest

The authors declare that they have no known competing financial interests or personal relationships that could have appeared to influence the work reported in this paper.

Data Availability

The data presented in this study will be made available on request from the corresponding author.

References

[1] European Commission and Directorate-General for Climate Action, Going climate-neutral by 2050 : a strategic long-term vision for a prosperous, modern, competitive and climate-neutral EU economy, Publications Office, 2019. doi:doi/10.2834/02074.

[2] B. Mathiesen, N. Bertelsen, N. Schneider, L. García, S. Paardekooper, J. Thellufsen, S. Djørup, Towards a decarbonised heating and cooling sector in Europe: Unlocking the potential of energy efficiency and district energy, Aalborg Universitet, 2019. Report.

[3] W. Zhong, J. Chen, Y. Zhou, Z. Li, X. Lin, Network flexibility study of urban centralized heating system: Concept, modeling and evaluation, Energy 177 (2019) 334–346. doi:10.1016/j.energy.2019.04.081.

[4] H. Lund, B. Möller, B. V. Mathiesen, A. Dyrelund, The role of district heating in future renewable energy systems, Journal of Energy 35 (2010) 1381–1390. doi:10.1016/j.energy.2009.11.023.

[5] M. Sayegh, P. Jadwiszczak, B. Axcell, E. Niemierka, K. Bryś, H. Jouhara, Heat pump placement, connection and operational modes in european district heating, Energy and Buildings 166 (2018) 122–144. doi:10.1016/j.enbuild.2018.02.006.

[6] H. Lund, P. A. Østergaard, M. Chang, S. Werner, S. Svendsen, P. Sorknæs, J. E. Thorsen, F. Hvelplund, B. O. G. Mortensen, B. V. Mathiesen, C. Bojesen, N. Duic, X. Zhang, B. Möller, The status of 4th generation district heating: Research and results, Energy 164 (2018) 147–159. doi:10.1016/j.energy.2018.08.206.

[7] H. Lund, S. Werner, R. Wiltshire, S. Svendsen, J. E. Thorsen, F. Hvelplund, B. V. Mathiesen, 4th generation district heating (4gdh): Integrating smart thermal grids into future sustainable energy systems, Energy 68 (2014) 1–11. doi:10.1016/j.energy.2014.02.089.

[8] Council of the European Union, European Parliament, Directive (EU) 2023/1791 of the European Parliament and of the Council of 13 September 2023 on energy efficiency and amending Regulation (EU) 2023/955 (recast) (Text with EEA relevance), Official Journal, L 231, 2023. URL: http://data.europa.eu/eli/dir/2023/1791/oj.

[9] E. Scoccimarro, O. Cattaneo, F. Mattion, A. Bizeul, A. Risquez, R. Quadrelli, Country-level energy demand for cooling has increased over the past two decades, Communications Earth & Environment 4 (2023) 110245. doi:10.1038/s43247-023-00878-3.

[10] J. R. Centre, I. for Environment, Sustainability, K. Mutka, P. Papillon, R. Kalf, G. Stryi-Hipp, W. Weiss, B. Sanner, A. Land, 2020-2030-2050, common vision for the renewable heating and cooling sector in Europe – European technology platform on renewable heating and cooling, Publications Office, 2011. doi:doi/10.2788/20474.

[11] A. M. Khourchid, S. B. Ajjur, S. G. Al-Ghamdi, Building cooling requirements under climate change scenarios: Impact, mitigation strategies, and future directions, Buildings 12 (2022). doi:10.3390/buildings12101519.

[12] F. Boudali Errebai, D. Strebel, J. Carmeliet, D. Derome, Impact of urban heat island on cooling energy demand for residential building in montreal using meteorological simulations and weather station observations, Energy and Buildings 273 (2022) 112410. doi:10.1016/j.enbuild.2022.112410.

[13] W. Gang, S. Wang, D. Gao, F. Xiao, Performance assessment of district cooling systems for a new development district at planning stage, Applied Energy 140 (2015) 33–43. doi:10.1016/j.apenergy.2014.11.014.

[14] U. Persson, E. Wiechers, B. Möller, S. Werner, Heat roadmap europe: Heat distribution costs, Energy 176 (2019) 604–622. doi:10.1016/j.energy.2019.03.189.

[15] S. Jacobs, M. De Pauw, S. Van Minnebruggen, S. Ghane, T. Huybrechts, P. Hellinckx, I. Verhaert, Grouped charging of decentralised storage to efficiently control collective heating systems: Limitations and opportunities, Energies 16 (2023). doi:10.3390/en16083435.

[16] P. A. Østergaard, A. N. Andersen, Economic feasibility of booster heat pumps in heat pump-based district heating systems, Journal of Energy 155 (2018) 921–929. doi:10.1016/j.energy.2018.05.076.

[17] X. Yang, H. Li, S. Svendsen, Energy, economy and exergy evaluations of the solutions for supplying domestic hot water from low-temperature district heating in denmark, Energy Conversion and Management 122 (2016) 142–152. URL: https://www.sciencedirect.com/science/article/pii/S0196890416304356. doi:10.1016/j.enconman.2016.05.057.

[18] C. Vering, L. Maier, K. Breuer, H. Krützfeldt, R. Streblow, D. Müller, Evaluating heat pump system design methods towards a sustainable heat supply in residential buildings, Applied Energy 308 (2022) 118204. doi:10.1016/j.apenergy.2021.118204.

[19] D. Blum, J. Arroyo, S. Huang, J. Drgoňa, F. Jorissen, H. T. Walnum, Y. Chen, K. Benne, D. Vrabie, M. Wetter, L. Helsen, Building optimization testing framework (boptest) for simulation-based benchmarking of control strategies in buildings, Journal of Building Performance Simulation 14 (2021) 586–610. doi:10.1080/19401493.2021.1986574.

[20] D. Wang, W. Zheng, Z. Wang, Y. Wang, X. Pang, W. Wang, Comparison of reinforcement learning and model predictive control for building energy system optimization, Applied Thermal Engineering 228 (2023) 120430. doi:10.1016/j.applthermaleng.2023.120430.

[21] H. Wang, L. Liu, L. Liu, Q. Cheng, Performance analysis of different air conditioning systems in apartment buildings under different climates in china, International Journal of Refrigeration 139 (2022) 192–203. doi:10.1016/j.ijrefrig.2022.04.007.

[22] T. Benakopoulos, W. Vergo, M. Tunzi, R. Salenbien, S. Svendsen, Overview of solutions for the low-temperature operation of domestic hot-water systems with a circulation loop, Energies 14 (2021) 3350. doi:10.3390/en14113350.

[23] W. Debacker, K. Allacker, C. Spirinckx, T. Geerken, F. De Troyer, Identification of environmental and financial cost efficient heating and ventilation services for a typical residential building in belgium, Journal of Cleaner Production 57 (2013) 188–199. doi:10.1016/j.jclepro.2013.05.037.

[24] A. Allouhi, M. Benzakour Amine, C. Reisch, Multi-objective optimization of solar energy systems for electricity and hot water generation in collective residential buildings considering the power-to-heat concept, Applied Thermal Engineering 230 (2023) 120658. doi:10.1016/j.applthermaleng.2023.120658.

[25] Council of the European Union, European Parliament, Directive (eu) 2018/844 of the european parliament and of the council of 30 may 2018 amending directive 2010/31/eu on the energy performance of buildings and directive 2012/27/eu on energy efficiency, Official Journal of the European Union, L156 61 (2018) 75–91. doi:http://data.europa.eu/eli/dir/2018/844/oj.

[26] G. Dermentzis, M. Magni, F. Ochs, W. Monteleone, B. Schaffer, Heat pump solutions in renovations of multi-storey buildings, in: CLIMA 2022 Conference: The 14th REHVA HVAC World Congress, REHVA, Rotterdam, The Netherlands, 2022, pp. 1–8. doi:10.34641/clima.2022.71.

[27] G. Martinopoulos, K. T. Papakostas, A. M. Papadopoulos, Comparative analysis of various heating systems for residential buildings in mediterranean climate, Energy and Buildings 124 (2016) 79–87. doi:10.1016/j.enbuild.2016.04.044.

[28] M. H. Abbasi, B. Abdullah, R. Castaño-Rosa, M. W. Ahmad, A. Rostami, A framework to identify and prioritise the key sustainability indicators: Assessment of heating systems in the built environment, Sustainable Cities and Society 95 (2023) 104629. doi:10.1016/j.scs.2023.104629.

[29] H. Jafaryeganeh, M. Ventura, C. Guedes Soares, Application of multi-criteria decision making methods for selection of ship internal layout design from a pareto optimal set, Ocean Engineering 202 (2020) 107151. doi:10.1016/j.oceaneng.2020.107151.

[30] M. Rodríguez-Pertuz, J. Terés-Zubiaga, A. Campos-Celador, I. González-Pino, Feasibility of zonal space heating controls in residential buildings in temperate climates: Energy and economic potentials in spain, Energy and Buildings 218 (2020) 110006. doi:10.1016/j.enbuild.2020.110006.

[31] B. van der Heijde, A. Vandermeulen, R. Salenbien, L. Helsen, Representative days selection for district energy system optimisation: a solar district heating system with seasonal storage, Applied Energy 248 (2019) 79–94. doi:10.1016/j.apenergy.2019.04.030.

[32] VLAIO, Instal 2020 project: Integraal ontwerp van installaties voor sanitair en verwarming (dutch), https://www.instal2020.be/, 2014-2018. VIS 135098.

[33] J. De Schutter, I. Verhaert, M. De Pauw, A methodology to generate realistic random behavior profiles for space heating and domestic hot water simulations, in: The REHVA Annual Meeting Conference: Low Carbon Technologies in HVAC, REHVA, Brussels, Belgium, 2018, pp. 1–8.

[34] F. Van Riet, Hydronic design of hybrid thermal production systems in buildings, PhD dissertation, University of Antwerp, 2019.

[35] S. Jacobs, F. Van Riet, I. Verhaert, A collective heat and cold distribution system with decentralized booster heat pumps: a sizing study., in: Building Simulation 2021: 17th Conference of IBPSA, volume 17, IBPSA, Bruges, Belgium, 1-3 September 2021, pp. 223–230. doi:10.26868/25222708.2021.30423.

[36] I. Verhaert, B. Bleys, S. Binnemans, E. Janssen, A methodology to design domestic hot water production systems based on tap patterns, in: CLIMA 2016 conference: REHVA 12th HVAC World Congress, REHVA, Aalborg, Denmark, 2016, pp. 1–8.

[37] ClimaWays BVBA, Collindi verwarmingssatellieten: geïndividualiseerde collectieve verwarmingssystemen (dutch), 2022. Datasheet.

[38] Solar Energy Laboratory Univ. of Wisconsin-Madison (SELUWM), TRNSYS 17 volume 4 mathematical reference: Type 60 (stratified fluid storage tank with internal heat exchangers), TRNSYS 17 4 (2009) 390–396.

[39] R. Zhang, D. Wang, Z. Yu, Y. Sun, H. Wan, Y. Liu, Q. Jiao, M. Gao, J. Fan, B. Lan, Dual-objective optimization of large-scale solar heating systems integrated with water-to-water heat pumps for improved techno-economic performance, Energy and Buildings 296 (2023) 113281. doi:10.1016/j.enbuild.2023.113281.

[40] F. Van Riet, G. Steenackers, I. Verhaert, A new approach to model transport delay in branched pipes, in: 10th International Conference on System Simulation in Buildings, Liège, Belgium, 2018, pp. 1–17.

[41] D. Brkić, Review of explicit approximations to the colebrook relation for flow friction, Journal of Petroleum Science and Engineering 77 (2011) 34–48. doi:10.1016/j.petrol.2011.02.006.

[42] T. Yang, W. Liu, G. J. Kramer, Q. Sun, Seasonal thermal energy storage: A techno-economic literature review, Renewable and Sustainable Energy Reviews 139 (2021) 110732. doi:10.1016/j.rser.2021.110732.

[43] R. Grosse, B. Christopher, W. Stefan, R. Geyer, S. Robbi, Long term (2050) projections of techno-economic performance of large-scale heating and cooling in the EU, Anticipation and foresight, Technical guidance KJ-NA-28859-EN-N, JRC Publications Repository, Luxembourg (Luxembourg), 2017. doi:10.2760/24422.

[44] The Danish Energy Agency and Energinet, Technology data for energy storage, https://ens.dk/en/our-services/projections-and-models/technology-data/technology-data-energy-storage, 2023. Datasheet - updated September 2023.

[45] T. Résimont, Strategic outline and sizing of district heating networks using a geographic information system, PhD dissertation, University of Liège, 2021.

[46] X. Yang, H. Li, S. Svendsen, Evaluations of different domestic hot water preparing methods with ultra-low-temperature district heating, Energy 109 (2016) 248–259. doi:10.1016/j.energy.2016.04.109.

[47] Vlaamse Statistische Autoriteit, Statistics flanders, https://www.vlaanderen.be/en/statistics-flanders/population/, 2023. [Online; accessed 20-March-2024].

[48] StatBel, Belgium in figures (population), https://statbel.fgov.be/en/themes/population/structure-population, 2023. [Online; accessed 20-March-2024].

[49] Vlaams Energie – en Klimaatagentschap, Bijlage v – bepalingsmethode epw 2022 (dutch), https://www.energiesparen.be/bouwen-en-verbouwen/epb-pedia/epb-regelgeving/energiebesluit/bijlage-v/, 2022. [Online; accessed 9-February-2022].

[50] Buildwise, Average weather profiles for Belgium, 2023. URL: http://

www.buildwise.be/nl/, the profiles were created by Buildwise as part of the IEA EBC Annex 80 project (https://annex80.iea-ebc.org/). Data are from the REMO15 model forced by MPI-M-MPI-ESM-LR. Accessed: 17-01-2023.

[51] C. Verhaeghe, S. Verbeke, A. Audenaert, A consistent taxonomic framework: towards common understanding of high energy performance building definitions, Renewable and Sustainable Energy Reviews 146 (2021) 111075. doi:10.1016/j.rser.2021.111075.